Virology 424 (2012) 56–66

Contents lists available at SciVerse ScienceDirect

Virology

journal homepage: www.elsevier.com/locate/yviro

O-sulfate groups of heparin are critical for inhibition of ecotropic murine leukemia virus infection by heparin

Yohei Seki [a], Misaho Mizukura [a], Tomomi Ichimiya [a], Yasuo Suda [b], Shoko Nishihara [a], Michiaki Masuda [c], Sayaka Takase-Yoden [a,*]

[a] Department of Bioinformatics, Faculty of Engineering, Soka University, Hachioji, Tokyo 192-8577, Japan
[b] Graduate School of Science and Engineering, Kagoshima University, Kagoshima 890-8580, Japan
[c] Department of Microbiology, Dokkyo Medical University School of Medicine, Tochigi 321-0293, Japan

ARTICLE INFO

Article history:
Received 3 September 2011
Returned to author for revision
27 November 2011
Accepted 28 November 2011
Available online 9 January 2012

Keywords:
Env protein
Heparin
Murine leukemia virus
Sulfation
Surface plasmon resonance

ABSTRACT

There is increasing evidence that soluble glycosaminoglycans such as heparin can interfere with the infectivity of various viruses, including ecotropic murine leukemia viruses (MLVs). The ecotropic MLV, Friend MLV (F-MLV) and the neuropathogenic variants A8 MLV and PVC-211 MLV, were susceptible to heparin-mediated inhibition of infection of NIH 3T3 cells. To investigate the interaction between the envelope glycoprotein (Env) of MLV and heparin, we prepared vesicular stomatitis virus-based pseudotyped viruses carrying the Env of F-, A8, or PVC-211 MLVs. Surface plasmon resonance analyses indicated that the Env of A8 and PVC-211 MLVs had a higher binding activity to heparin than that of F-MLV. We examined the influence of *N*- or *O*-sulfation of heparin on binding activity to Env and on the inhibition of the infectivity of MLV and pseudotyped viruses carrying Env. This analysis indicated that the *O*-sulfate groups of heparin play a major role in determining Env-dependent inhibitory effects.

Introduction

Previous studies have shown that soluble glycosaminoglycans (GAGs), such as heparin, inhibit the infectivity of ecotropic murine leukemia virus (MLV) (Batra et al., 1997; Guibinga et al., 2002; Jinno-Oue et al., 2001; Le Doux et al., 1996, 1999; Masuda et al., 1997; Walker et al., 2002). Jinno-Oue et al. (2001) found that heparin influences Env-dependent attachment of the virus to the cell surface. By contrast, Walker et al. (2002) and Guibinga et al. (2002) reported that heparin inhibits Env-independent interaction of MLV with target molecules on the cell surface. Infection by ecotropic MLV is mediated by the binding of the viral Env protein to the rodent ortholog of cationic amino acid transporter 1 (CAT-1), which serves as the specific cellular receptor (Albritton et al., 1989; Kim et al., 1991; Wang et al., 1991). Although the Env-receptor interaction appears to be required for membrane fusion and entry of the viral capsid, it has been reported that initial attachment of a retroviral particle to the cell surface can take place in a receptor-independent manner (Guibinga et al., 2002; Pizzato et al., 1999; Walker et al., 2002). The fact that soluble GAGs, such as heparin, inhibit MLV infectivity suggests that cell surface GAGs, such as heparan sulfate, might be involved in the initial attachment (Batra et al., 1997; Guibinga et al., 2002; Jinno-Oue et al., 2001; Le Doux et al., 1996, 1999; Masuda et al., 1997; Walker et al., 2002). Similarly, it has been shown that infection by other enveloped viruses, such as herpes viruses (Neyts et al., 1992; Secchiero et al., 1997; WuDunn and Spear, 1989), respiratory syncytial virus (Krusat and Streckert, 1997) and human immunodeficiency virus (HIV) (Mondor et al., 1998; Patel et al., 1993), are inhibited by heparin, and that cell surface attachment of these viruses involves cell surface GAGs. Thus, the interaction of viral particles with soluble and cell surface GAGs is an important issue for virology in general.

In the present study, we initially investigated the influence of heparin on infection of ecotropic MLVs including Friend MLV (F-MLV) clone 57 (Oliff et al., 1980) and its neuropathogenic variants, A8 MLV (Takase-Yoden and Watanabe, 1997; Watanabe and Takase-Yoden, 1995) and PVC-211 MLV (Kai and Furuta, 1984; Masuda et al., 1992). The infection of neonatal rats with A8 or PVC-211 MLV induces spongiform neurodegeneration without inflammatory infiltrates. The primary determinant for neuropathogenicity of these viruses has been identified as Env. Comparison of the amino acid sequences of A8-Env and PVC-211-Env showed that only 3 of the 676 amino acids differ. F-MLV is non-neuropathogenic and F-Env shows differences at 26 of the 676 amino acids compared to A8-Env. Here, we performed surface plasmon resonance (SPR) analyses to compare the binding activities to heparin of pseudotyped viral particles carrying Env of ecotropic MLVs. To our knowledge, this is the first time that SPR technology has been applied in a quantitative analysis of

* Corresponding author. Fax: +81 42 691 2375.
E-mail address: takase@soka.ac.jp (S. Takase-Yoden).

0042-6822/$ – see front matter © 2011 Elsevier Inc. All rights reserved.
doi:10.1016/j.virol.2011.11.030

the interaction between viral particles carrying MLV Env and heparin. Heparin is a linear polysaccharide composed of α1-4 linked disaccharide repeating units. The most common unit contains 2-*O*-sulfated iduronic acid and 6-*O*-sulfated, *N*-sulfated glucosamine. The negatively-charged sulfate groups of heparan sulfate (which is structurally related to heparin) are thought to play an important role in its biological activity, such as fibroblast growth factor (FGF) signaling, and to act as an entry receptor for herpes simplex virus type 1 (Capila and Linhardt, 2002; Copeland et al., 2008; Shukla et al., 1999; Xia et al., 2002; Ye et al., 2001). We also examined the relative importance of *N*- or *O*-sulfation of heparin for its inhibitory effects on infection by ecotropic MLVs and on the binding activities to viral particles using chemically modified heparins: *N*-acetylheparin (NA-H), which has diminished *N*-sulfation; de-*N*-sulfated heparin (dNS-H), which completely lacks *N*-sulfation; and *N*-acetyl-de-*O*-sulfated heparin (NAdOS-H), which has markedly diminished *N*-sulfation and completely lacks *O*-sulfation. Taken together, the present investigations have characterized the inhibitory activities of heparin against ecotropic MLV infection of NIH 3T3 cells, while the SPR analysis showed that the binding activity of ecotropic MLV with heparin may be determined by Env amino acid sequences. We also demonstrate that the *O*-sulfate groups of heparin play a major role in inhibiting the infectivity of ecotropic MLV on cells in an Env-dependent manner. The possible mechanisms of the inhibition of heparin against viral infection and the implications of heparan sulfate on the cell surface are discussed.

Results

Inhibition of ecotropic MLV infection by heparin and its derivatives

We compared the effects of heparin and its derivatives on the infectivity of F-, A8, and PVC-211 MLVs using viruses that had been pre-incubated with various concentrations of heparin, or one of the derivatives, in the absence of polybrene. After this pre-incubation step, the virus-heparin or virus-derivative mixture was inoculated onto NIH 3T3 cells at a multiplicity of infection (MOI) of 1 in the presence of 10 μg/ml polybrene. We used polybrene for viral infection, because MLV infections are usually carried out in the presence of polybrene to enhance infection. After 72 h, viral production was evaluated by measuring virion-associated reverse transcriptase (RT) activities in the culture supernatants.

Pre-incubation of the viruses with heparin at concentrations greater than 1 μg/ml resulted in a dose-dependent decrease in viral production (Fig. 1A). The 50% inhibitory dose (ID_{50}) values of heparin for F-, A8, and PVC-211 MLVs were 12.7 ± 4.5, 8.5 ± 0.9, and 13.0 ± 3.3 μg/ml, respectively; these values were not significantly different (Table 1). The structure of the most common disaccharide unit of heparin is composed of 2-*O*-sulfated iduronic acid and 6-*O*-sulfated, *N*-sulfated glucosamine (Fig. 1E). To investigate whether differences in the sulfation patterns of heparin affect the ability to inhibit ecotropic MLV infection, we pre-incubated viruses with a heparin derivative: NAdOS-H, which has markedly diminished *N*-sulfation and no *O*-sulfation; NA-H, which has diminished *N*-sulfation; or dNS-H, which completely lacks *N*-sulfation. NAdOS-H did not show inhibitory effects on infection of NIH 3T3 cells with F-, A8, or PVC-211 MLV even at a concentration of 1000 μg/ml (Fig. 1B and Table 1). In contrast, NA-H inhibited production of F-, A8, and PVC-211 MLVs in infected NIH 3T3 cells, with ID_{50} values of 54.5 ± 4.1, 62.1 ± 2.5, and 53.7 ± 2.8 μg/ml, respectively (Fig. 1C and Table 1); these values were significantly higher than for heparin ($P<0.001$). dNS-H also inhibited infection of NIH 3T3 cells with F-, A8, and PVC-211 MLVs, with ID_{50} values of 76.8 ± 3.9, 65.4 ± 2.3, and 72.4 ± 4.2 μg/ml, respectively (Fig. 1D and Table 1). The ID_{50} values for dNS-H were significantly higher than those of heparin ($P<0.001$).

Preparation of vesicular stomatitis virus (VSV)-based pseudotyped viruses carrying ecotropic MLV Env

Previous studies suggested that heparin affects ecotropic MLV infection during the early steps of viral replication. We used pseudotyped viruses bearing Env to analyze the effects of heparin on the viral replication process from the attachment to gene expression steps. We also sought to clarify the contribution of Env of ecotropic MLV to the inhibitory effects of heparin against viral infectivity by examining this response in the absence of other retroviral proteins, such as Gag and Pol, that might influence heparin-mediated reduction in infectivity. To this end, we prepared VSV based-pseudotyped viruses carrying the Env of F-, A8, or PVC-211 MLV (VSV/F-Env, VSV/A8-Env, and VSV/PVC-211-Env, respectively) using 293T cells.

Initially, we performed a Western blot analysis using an anti-Env antibody to examine whether Env protein is normally expressed in the 293T cells transfected with F-, A8-, and PVC-211-Env expression vectors, and compared the expression levels of Env in these cells. In the transfected 293T cells, the primary product observed was gp70, although gpr85 was also detectable (lanes 1–3 in Fig. 2). The expression levels of Env protein were similar in cells transfected with F-, A8-, and PVC-211-Env expression vectors. The Env-expressing cells were infected with recombinant VSV, which has the green fluorescence protein (GFP) gene in place of the viral G protein gene, and VSV-pseudotyped viruses carring Env were obtained. As a control, VSV viruses-like particles lacking Env (VSV/ΔEnv) were also obtained as described in the Materials and methods section. Next, we compared the amount of Env protein packaged in VSV-pseudotyped viruses among VSV/F-Env, VSV/A8-Env, and VSV/PVC-211-Env. In total, 2×10^5 infectious units of VSV/F-Env, VSV/A8-Env, and VSV/PVC-211-Env were spun down and the precipitates were used in a Western blot analysis. With regard to viral particles, gp70 was observed, and the amount of Env protein showed no appreciable differences among the virions (lanes 5–7 in Fig. 2).

Inhibitory effects of heparin and its derivatives on the infectivity of VSV-based pseudotyped viruses carrying ecotropic MLV Env

We examined the inhibitory effects of heparin and its derivatives on the infectivity of VSV-based pseudotyped viruses carrying ecotropic MLV Env. VSV/F-Env, VSV/A8-Env, and VSV/PVC-211-Env were pre-incubated with various concentrations of heparin, or a derivative, in the absence of polybrene, and then inoculated onto NIH 3T3 cells at an MOI of 1 in the presence of 10 μg/ml polybrene. After 16 h, GFP-positive cells were counted by fluorescence-activated cell sorting (FACS) in order to evaluate viral infectivity. Heparin was found to inhibit infection of NIH 3T3 cells with VSV/F-Env, VSV/A8-Env, and VSV/PVC-211-Env (Fig. 3A) with ID_{50} values of 7.0 ± 0.3, 8.0 ± 0.3, and 7.4 ± 0.4 μg/ml, respectively (Table 2). Although NAdOS-H did not inhibit infectivity of VSV/F-Env, VSV/A8-Env, or VSV/PVC-211-Env on NIH 3T3 cells (Fig. 3B and Table 2), high concentrations of NA-H or dNS-H did show inhibition of infection of NIH 3T3 cells (Figs. 3C and D). The ID_{50} values of NA-H (50.1 ± 3.9, 53.4 ± 2.6, and 50.8 ± 3.7 μg/ml for VSV/F-Env, VSV/A8-Env, and VSV/PVC-211-Env, respectively) and of dNS-H (67.8 ± 1.5, 64.8 ± 2.0, and 71.5 ± 1.8 μg/ml for VSV/F-Env, VSV/A8-Env, and VSV/PVC-211-Env, respectively) were significantly higher than those of heparin ($P<0.001$) (Table 2).

We also sought to compare the effects of heparin and its derivatives on the infectivity of ΔEnv-VSV-pseudotyped viruses. However, the efficiency of GFP gene transduction of the cells with the ΔEnv-VSV-pseudotyped viruses was too low to allow a reliable comparison to be carried out.

SPR analysis of the direct interactions of ecotropic MLV Env with heparin or its derivatives

In order to analyze direct interactions between Env and heparin, we measured the binding activities of VSV/F-Env, VSV/A8-Env, and

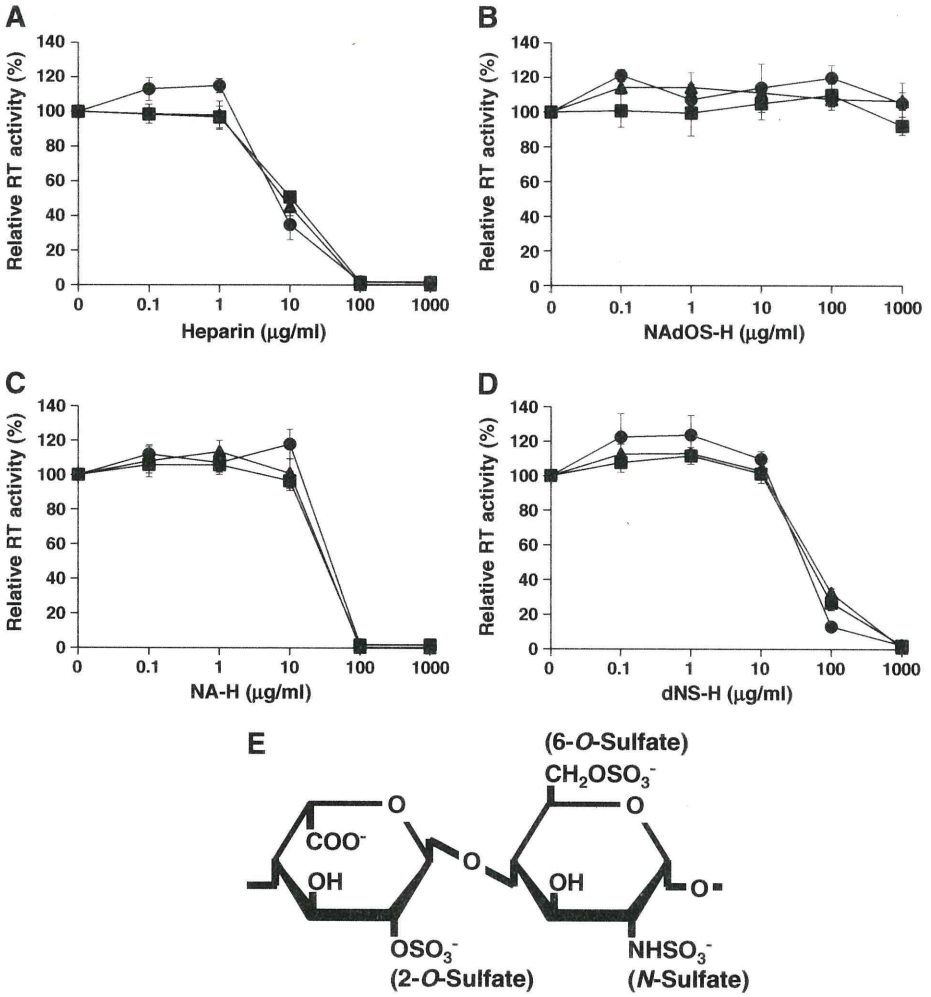

Fig. 1. Inhibitory activities of heparin and three derivatives against production of retroviruses in NIH 3T3 cells. F- (triangle), A8 (circle), and PVC-211 (square) MLVs were pre-incubated with various concentrations of heparin (A), NAdOS-H (*N*-acetyl-de-*O*-sulfated heparin) (B), NA-H (*N*-acetylheparin) (C), or dNS-H (de-*N*-sulfated heparin) (D) for 1 h at 37 °C in the absence of polybrene. The virus–heparin mixture was then inoculated onto NIH 3T3 cells in the presence of 10 μg/ml polybrene. After incubation for 1 h at 37 °C, the cells were washed three times with FCS-free DMEM and fresh culture medium was added. After 72 h, virion-associated RT activity in the culture supernatants was measured by an RT assay as described in the Materials and methods section. The mean values of 4 independent experiments and SEM are shown. (E) Schematic diagram of the major disaccharide repeating units of heparin. The most common disaccharide unit of heparin is composed of 2-*O*-sulfated iduronic acid and 6-*O*-sulfated, *N*-sulfated glucosamine.

VSV/PVC-211-Env to a heparin-immobilized chip (Heparin chip) by SPR. The SPR analyses were performed in the absence of polybrene; this protocol was adopted because in the experiments on inhibition of viral infection by heparin (Figs. 1 and 3), the viruses were pre-incubated with heparin in the absence of polybrene. Two different preparations of each pseudotyped virus were used for the analysis.

Table 1
ID_{50} of heparin and three derivatives against infection of MLVs into NIH 3T3 cells.

Reagents	Viruses		
	F	A8	PVC-211
Heparin	12.7 ± 4.5[a]	8.5 ± 0.9[a]	13.0 ± 3.3[a]
NAdOS-H	>1000	>1000	>1000
NA-H	54.5 ± 4.1	62.1 ± 2.5	53.7 ± 2.8
dNS-H	76.8 ± 3.9	65.4 ± 2.3	72.4 ± 4.2

ID_{50} values (μg/ml) were calculated from the data shown in Fig. 1. The mean values (and SEMs) of 4 independent experiments are shown. Statistical comparison was performed using the t test. NAdOS-H: *N*-acetyl-de-*O*-sulfated heparin; NA-H:*N*-acetyl-heparin; dNS-H: de-*N*-sulfated heparin.

[a] $P<0.001$ vs NA-H and dNS-H in each virus.

Env-deficient VSV-like particles (VSV/ΔEnv) and culture supernatant from 293T cells (Mock) were used as negative controls. Typical sensorgrams of the binding of the samples to the Heparin chip are shown in the top column of Fig. 4A. The flow of the viral particles, at various concentrations, across the Heparin chip was started at 0 s, and flow of the washing buffer was started at 300 s. Since the binding of virus to the Heparin chip appeared to reach equilibrium at 450 s, the Δdeg value at 450 s was selected as reflecting binding activity and plotted as shown in the top column of Fig. 4B. The results indicated that VSV-based pseudotyped viruses were bound to the Heparin chip in a dose-dependent manner. The binding activities of VSV/A8-Env and VSV/PVC-211-Env were clearly higher than that of VSV/F-Env, which exhibited higher binding activity than the negative controls. When viruses were saturated with heparin prior to SPR analysis, binding to the Heparin chip was inhibited (data not shown).

The binding activities of the VSV-based pseudotyped viruses to NAdOS-H or dNS-H immobilized on SPR sensor chips (NAdOS-H or dNS-H chips, respectively) were also examined (middle and bottom columns of Figs. 4A and B). We found that VSV-based pseudotyped viruses showed dose-dependent binding to the NAdOS-H or dNS-

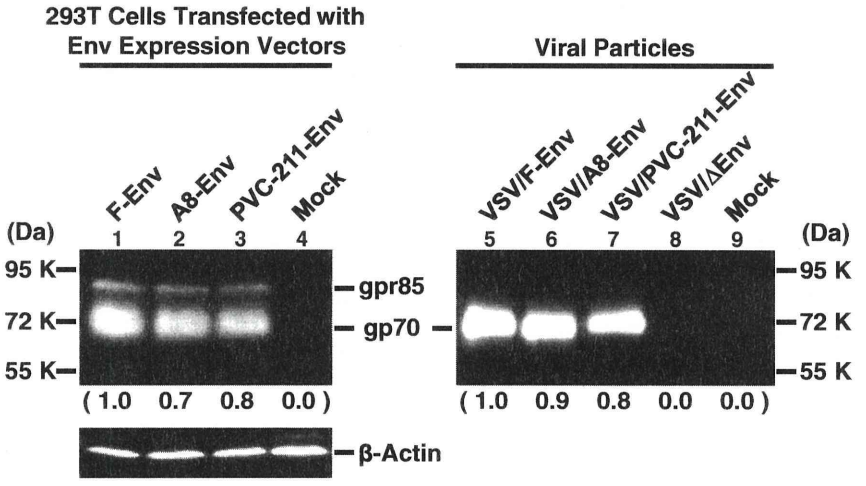

Fig. 2. Western blot analysis of the expression levels of Env in 293T cells transfected with Env expression vectors and VSV-pseudotyped virus particles. Lanes 1–3: 293T cells transfected with Env expression vectors. Lane 4: Mock-transfected 293T cells. Lanes 5–7: VSV-pseudotyped virus particles carring Env. 2×10^5 infectious units of viruses were applied to the Western blot. Details are given in the Materials and methods section. Lane 8: Env-deficient VSV-like particles prepared as described in the Materials and methods section. Lane 9: culture supernatant from 293T cells (used in the SPR analysis as a Mock control) was prepared as described in the Materials and methods section. To detect the Env protein, anti-SU (gp70) was used. Relative amount of Env protein is shown in parentheses. The expression levels of Env protein of transfected 293T cells were normalized against the intensity of the beta-actin band and are shown relative to the cell transfected with F-Env expression vector. The amount of Env protein in virions is shown relative to the VSV/F-Env. This figure is representative of repeat experiments. Experiments with each sample were performed twice and similar results were obtained.

H chips. The binding activities of VSV/A8-Env and VSV/PVC-211-Env to NAdOS-H or dNS-H were higher than those of VSV/F-Env. The binding activities of VSV/A8-Env and VSV/PVC-211-Env to NAdOS-H were clearly lower than those to heparin, but were similar or slightly lower than those to dNS-H. The binding activities of VSV/F-Env to NAdOS-H were slightly lower than those to heparin, and were not significantly different to those for dNS-H. Although NAdOS-H did not show any detectable inhibition of the infectivity of ecotropic MLV or VSV-based pseudotyped viruses carrying ecotropic Env, the binding activities of VSV/F-Env, VSV/A8-Env, and VSV/PVC-211-Env to this ligand appeared to be comparable to those to dNS-H.

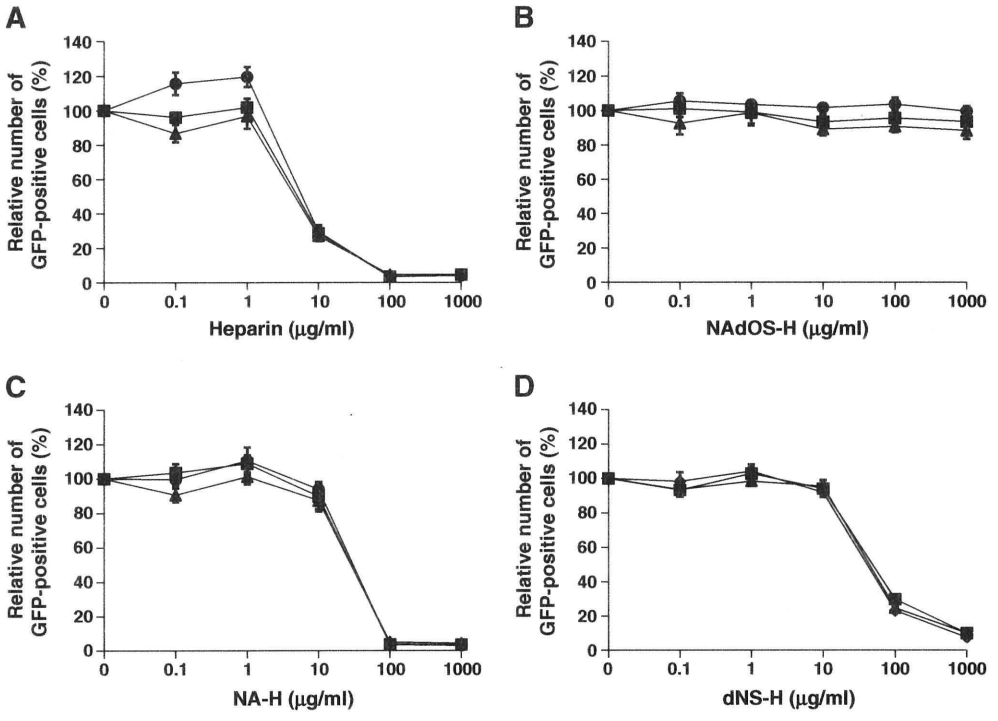

Fig. 3. Inhibitory activities of heparin and three derivatives against infection of VSV based-pseudotyped viruses carrying Env into NIH 3T3 cells. VSV/F-Env (triangle), VSV/A8-Env (circle), and VSV/PVC-211-Env (square) were pre-incubated with various concentrations of heparin (A), NAdOS-H (*N*-acetyl-de-*O*-sulfated heparin) (B), NA-H (*N*-acetylheparin) (C), or dNS-H (de-*N*-sulfated heparin) (D) for 1 h at 37 °C in the absence of polybrene. Then the virus–heparin mixture was inoculated onto NIH 3T3 cells in the presence of 10 μg/ml polybrene. After 16 h, GFP-positive cells were counted by FACS analyses. The mean values of 4 independent experiments and SEM are shown.

Table 2
ID_{50} of heparin and three derivatives against infection of VSV based-pseudotyped viruses carrying Env of MLV into NIH 3T3 cells.

Reagents	VSV based-pseudotyped viruses		
	VSV/F-Env	VSV/A8-Env	VSV/PVC-211-Env
Heparin	7.0 ± 0.3[a]	8.0 ± 0.3[a]	7.4 ± 0.4[a]
NAdOS-H	>1000	>1000	>1000
NA-H	50.1 ± 3.9	53.4 ± 2.6	50.8 ± 3.7
dNS-H	67.8 ± 1.5	64.8 ± 2.0	71.5 ± 1.8

ID_{50} values (μg/ml) were calculated from the data shown in Fig. 3. The mean values (and SEMs) of 4 independent experiments are shown. Statistical comparison was performed using the *t* test. NAdOS-H: *N*-acetyl-de-*O*-sulfated heparin; NA-H:*N*-acetyl-heparin; dNS-H: de-*N*-sulfated heparin.

[a] $P<0.001$ vs NA-H and dNS-H in each virus.

Effect of polybrene on heparin-induced inhibition of MLV infection

In order to determine the effect of polybrene on the inhibitory activity of heparin against MLV infection, we performed experiments in the presence and absence of polybrene. Firstly, we examined the effects of polybrene on MLV infection at an MOI of 1. In the absence of polybrene, at 72 h post-infection, viral production of MLVs was undetectable level by an RT assay; at 96 h post-infection, viral production was detectable but was 10- to 50-fold lower than in the presence of polybrene (data not shown). In the presence of polybrene, viral production at 96 h post-infection was higher than at 72 h post-infection. Therefore, we evaluated viral production at 96 h post-infection in the following experiment. F-, A8, and PVC-211 MLVs were pre-incubated with various concentrations of heparin in the absence of polybrene, and then inoculated onto NIH 3T3 cells at an MOI of 1 either in the presence of 10 μg/ml polybrene or in its absence; viral production was evaluated at 96 h. In the presence of polybrene, the ID_{50} values of heparin for F-, A8, and PVC-211 MLVs were 44.4 ± 6.7, 47.9 ± 0.8, and 49.6 ± 2.2 μg/ml, respectively; these values were not significantly different (Fig. 5A and Table 3). The ID_{50} values in this experiment are higher than those shown in Fig. 1A and Table 1 due to differences in culture time; nevertheless, the inhibition curves in Fig. 5A are similar to those in Fig. 1A. In the absence of polybrene, the ID_{50} values of heparin for F-, A8, and PVC-211 MLVs were 0.56 ± 0.08, 0.61 ± 0.10, and 0.60 ± 0.05 μg/ml, respectively (Fig. 5B and Table 3); these values are not significantly different. However, these values are significantly lower than those in the presence of polybrene ($P<0.001$).

We also attempted to examine the effects of polybrene on the inhibitory activity of heparin against infection of NIH 3T3 cells by VSV-pseudotyped viruses. However, the efficiency of GFP gene transduction of the cells with the pseudotyped viruses in the absence of polybrene was too low to allow the effects of heparin to be reliably compared (data not shown).

Discussion

Soluble GAGs, such as heparin, have been shown to inhibit infection by MLV (Guibinga et al., 2002; Jinno-Oue et al., 2001; Walker et al., 2002). It has been reported that this inhibitory effect is determined by a number of factors: GAG concentration; electrostatic charge on the GAG; the affinity of the virus to the GAG; the cells from which the viruses are produced; and the cell type infected with the viruses. In this study, we examined the effects of soluble GAGs on the ability of ecotropic MLVs produced by NIH 3T3 cells to infect NIH 3T3 cells. Jinno-Oue et al. (2001) showed that, in the absence of polybrene, low concentrations of heparin (up to 100 μg/ml) enhanced the infectivity of F- and PVC-211 MLVs, whereas higher concentrations inhibited infectivity. In contrast, we found that 0.1 μg/ml of heparin did not affect the infectivity of F-, A8, and PVC-211 MLVs in the absence of polybrene; however, concentrations greater than 1 μg/ml, heparin inhibited infectivity (Fig. 5B). In the presence of polybrene, we found that 1 μg/ml or less of heparin did not affect the infectivity of F-, A8, and PVC-211 MLVs; at concentrations greater than 10 μg/ml, however, heparin inhibited infectivity in a dose-dependent manner (Figs. 1A and 5A). The apparent lack of any enhancing effects of heparin on ecotropic MLV infectivity in the present study may be due to differences in experimental conditions. Thus, the discrepant results in this and the previous study might be a consequence of using different cell types in which to measure viral infectivities. Jinno-Oue et al. (2001) used Rat-1 and primary rat brain capillary endothelial cells (BCEC) as target cells, while we used mouse NIH 3T3 cells.

Walker et al. (2002) and Guibinga et al. (2002) reported that the cell surface attachment of Env-deficient retrovirus-like particles was inhibited by heparin, suggesting that heparin inhibits Env-independent interaction of MLV with target molecules on the cell surface. By contrast, Jinno-Oue et al. (2001) showed that subtle changes in the Env protein amino acid sequences, which generated a heparin-binding site(s), could affect the heparin-binding affinity of the viruses and the susceptibility of the viruses to the effects of heparin. Thus, it is likely that heparin influences not only Env-independent attachment, but also Env-dependent attachment of the virus to the cell surface. In our present study, the binding to heparin by VSV-based pseudotyped viruses carrying the Env of F-, A8, or PVC-211 MLVs was quantitatively examined by SPR analysis. To our knowledge, the present study is the first to quantitatively compare heparin binding activities of Env of different ecotropic MLVs using SPR technology. Our results indicated that the binding activities of VSV based-pseudotyped viruses carrying the Env of ecotropic MLVs were higher than that of the Env-deficient virus-like particle, and that the Env sequence influenced the binding activity of the pseudotyped viruses to heparin (Figs. 4 and 6). Therefore, the results strongly suggest that the Env per se of these ecotropic MLVs can directly interact with heparin. PVC-211-Env exhibited the highest heparin binding activity, followed by A8-Env, and then F-Env (Fig. 4). These results are consistent with those of a previous study in which heparin agarose was used to assess the heparin binding activities of F-MLV and PVC-211 MLV (Jinno-Oue et al., 2001). F-Env, which showed the lowest binding activity to heparin, had 26 amino acid substitutions compared to A8-Env (Fig. 6). By contrast, A8-Env and PVC-211-Env showed similar binding activities and differed by only 3 amino acids (Fig. 6). The consensus sequences for the heparin-binding domain (HBD) are XBBXBX and XBBBXXBX, where X represents any amino acid and B indicates a basic amino acid (Cardin and Weintraub, 1989). A stretch of 6 amino acids from Ser^{124} to Glu^{129} in the receptor-binding domain (RBD) of F-Env constitutes a putative HBD. However, a previous study suggested that this sequence did not function as an HBD (Jinno-Oue et al., 2001). Compared to F-Env, the substitution of Glu^{129} by Lys in PVC-211-Env generated an additional, overlapping HBD from Pro^{127} to Ser^{132}. This new HBD has been suggested to contribute to the high binding ability of PVC-211 MLV for heparin. Intriguingly, the amino acids at positions 124 to 132 of A8-Env are identical to those of F-Env, and thus A8-Env has only one putative HBD that might not be functional. Therefore, the number of HBDs cannot explain the difference in binding activities of A8-Env and F-Env to heparin. Recently, the heparin binding activities of wild-type and mutant gp120 of HIV-1 were studied using SPR-based binding assays (Crublet et al., 2008). Four new HBDs were identified in the V2 and V3 loops, in the C-terminal domain, and within the CD4-induced bridging sheet. Three of these HBDs were found in domains of the protein that are involved in co-receptor recognition. In particular, Arg^{419}, Lys^{421}, and Lys^{432}, which directly interact with the co-receptor, are targeted by heparin, suggesting that these basic amino acids are important for the interaction with heparin. In contrast to F-Env, which has Gln^{61} and Ser^{80} in the variable region A (VRA) of RBD, both A8-Env and PVC-211-Env have Arg^{61} and Arg^{80} in common (Fig. 6). Therefore, we suggest that

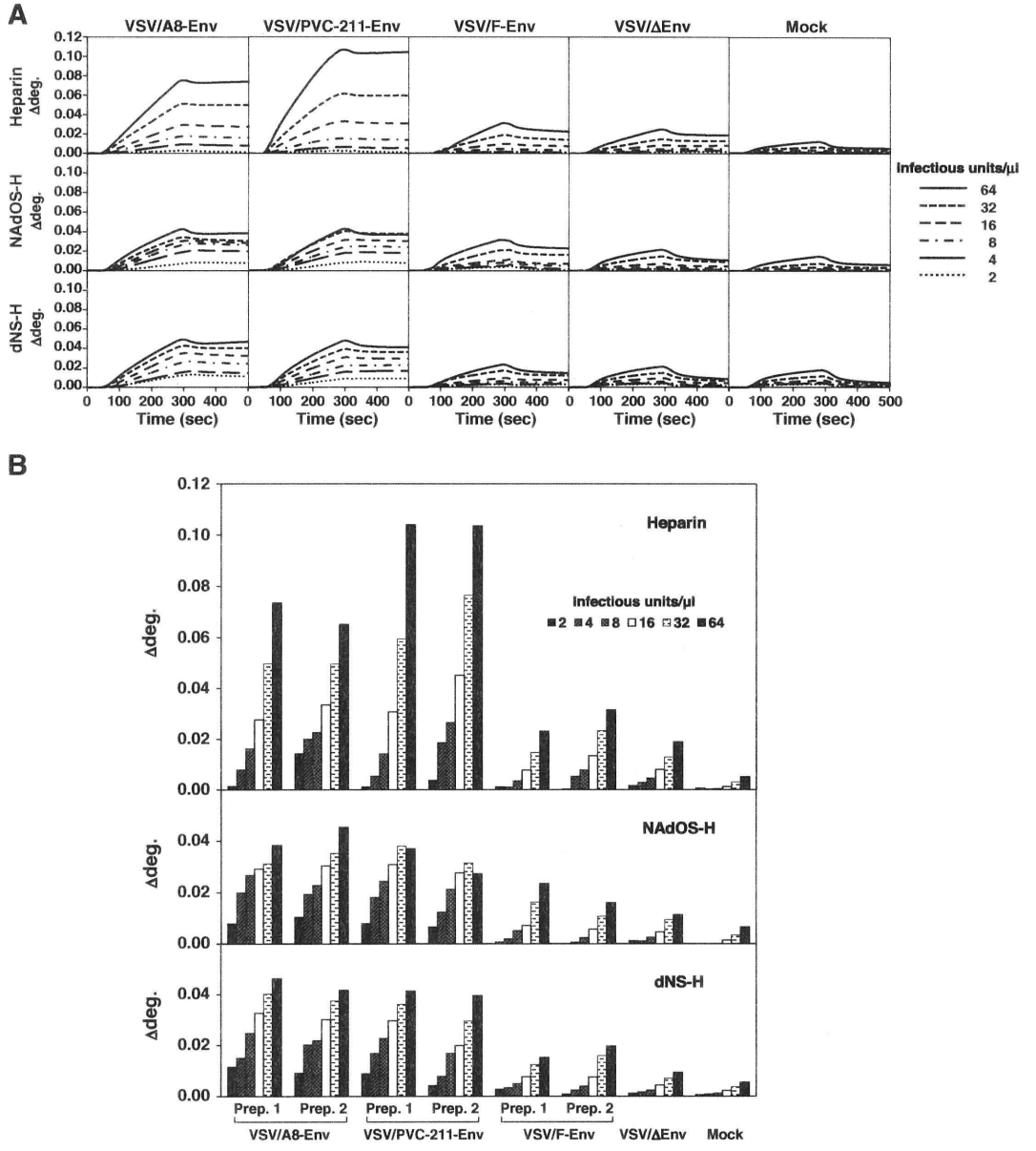

Fig. 4. SPR analysis of the binding of VSV based-pseudotyped viruses carrying Env of F- (VSV/F-Env), A8 (VSV/A8-Env), or PVC-211 MLV (VSV/PVC-211-Env) to heparin, NAdOS-H (*N*-acetyl-de-*O*-sulfated heparin), or dNS-H (de-*N*-sulfated heparin) immobilized on SPR sensor chips. Two independent preparations (Prep. 1 and Prep. 2) of VSV/F-Env, VSV/A8-Env, and VSV/PVC-211-Env were tested. (A) SPR sensorgrams of viral particles of Prep. 1 for the Heparin chip, the NAdOS-H chip, or the dNS-H chip. (B) The equilibrium level of binding of viral particles to the Heparin chip, the NAdOS-H chip, or the dNS-H chip at 450 s. VSV/ΔEnv: Env-deficient VSV-like particles; Mock: culture supernatants of 293T cells. 1×10^6 infectious units of VSV based-pseudotyped viruses carrying Env were prepared and treated for SPR analysis as described in the Materials and methods section. VSV/ΔEnv and Mock controls were prepared as described in the Materials and methods section. The aliquots from both controls were equivalent in volume to those from the culture supernatants of VSV/Env-producing cells, which contained 1×10^6 infectious units, and were treated in the same manner.

these two residues in A8- and PVC-211-Env might contribute to the higher heparin-binding activity. Furthermore, Lys^{129} is present only in PVC-211-Env and may be responsible for the additional heparin-binding activity.

Although PVC-211-Env had the highest heparin binding activity, followed by A8-Env, and then F-Env (Fig. 4), the ID_{50} values of heparin for infection by PVC-211, A8, or F-MLV were not significantly different (Fig. 1 and Table 1). Similarly, the ID_{50} values of heparin for infection of VSV-based pseudotyped viruses bearing PVC-211-, A8-, or F-Env were not significantly different (Fig. 3 and Table 2). The reasons why the estimates for inhibition of viral infection do not correlate with those from the SPR analyses are not clear, but the following possibilities could be suggested. First, the relatively low binding activity of Env to heparin, which was observed in the SPR analysis of F-Env, might be sufficient to block viral infection. Second, the SPR analysis might be more sensitive to heparin-binding activity than the inhibition assay of viral infectivity. In the SPR analysis, viral particles bind to heparin immobilized to a chip, and then excess and low-affinity viral particles are washed out. In contrast, in the inhibition assay, small soluble molecules of heparin bind to the Env of viruses, and thus relatively low-affinity binding between heparin and Env could have a significant effect on viral

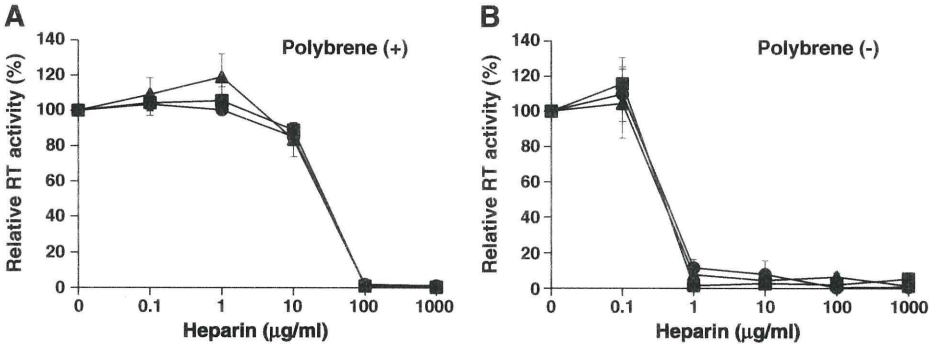

Fig. 5. Effects of polybrene on inhibitory activities of heparin against MLV infection. F- (triangle), A8 (circle), and PVC-211 (square) MLVs were pre-incubated with various concentrations of heparin for 1 h at 37 °C in the absence of polybrene. Then, the virus–heparin mixture was inoculated onto NIH 3T3 cells in the presence of 10 μg/ml polybrene (A) or in its absence (B). After incubation for 1 h at 37 °C, the cells were washed three times with FCS-free DMEM and fresh culture medium was added. After 96 h, virion-associated RT activity in the culture supernatants was measured by an RT assay as described in the Materials and methods section. The mean values of 4 independent experiments and SEM are shown.

infection. Third, we cannot exclude the possibility that heparin might affect viral replication steps except for attachment. Although we used VSV-pseudotyped viruses carrying Env for the inhibition assay against viral infection, the assay did not distinguish rigorously between viral attachment and alternative steps in infection, such as entry and gene expression. Therefore, heparin might not only influence viral attachment but also entry and gene expression, with the result that the ID_{50} values for viral infection are similar among the viruses despite the fact that they carry different Envs.

Heparin is a highly sulfated polysaccharide with a negative charge and its most common disaccharide unit is composed of 2-*O*-sulfated iduronic acid and 6-*O*-sulfated, *N*-sulfated glucosamine (Fig. 1E). Sulfation of heparan sulfate, which is structurally related to heparin, is thought to play an important role in its biological activity such as FGF signaling and its ability to act as an entry receptor for herpes simplex virus type 1 (Capila and Linhardt, 2002; Copeland et al., 2008; Shukla et al., 1999; Xia et al., 2002; Ye et al., 2001). It has also been shown that the chemical structure of the carbohydrate unit constituting the GAG backbone is an important determinant for the ability of the GAG to inhibit retroviral infection (Jinno-Oue et al., 2001; Walker et al., 2002). By comparing the effects of heparin and dNS-H, Jinno-Oue et al. (2001) concluded that *N*-sulfation of GAG is important for the effects on infectivity of ecotropic MLVs. In this study, NA-H, which has diminished *N*-sulfation, and dNS-H, which completely lacks *N*-sulfation, were shown to be less effective than heparin in inhibiting infection of NIH 3T3 cells by pseudotyped viruses carrying ecotropic MLV Env (Fig. 3 and Table 2). We have, therefore, confirmed that *N*-sulfation of GAG plays an important role in the inhibition of ecotropic MLV infection. In addition, NAdOS-H, which has markedly diminished *N*-sulfation and completely lacks *O*-sulfation, did not significantly alter infectivity of pseudotyped viruses on NIH 3T3 cells (Fig. 3). Comparison of dNS-H and NAdOS-H strongly suggests that the *O*-sulfate groups of GAG are also required for the inhibitory effects on MLV infection. Intriguingly, the results of the SPR analysis indicated that NAdOS-H, which failed to inhibit ecotropic MLV infection, binds to F-, A8-, and PVC-211-Env at levels comparable to those of dNS-H, which unequivocally exhibited inhibitory effects on viral infection. Therefore, binding of GAG to the viral Env may be essential, but not sufficient, for inhibition of Env-dependent MLV attachment to the cell surface. Previous studies have highlighted the importance of the *O*-sulfate group of heparin for its inhibitory activities against infection by pseudorabies virus (Trybala et al., 1996), herpes simplex virus (Trybala et al., 2000), and HIV (Rider et al., 1994). In contrast, *N*-sulfation of heparin is required for inhibition of respiratory syncytial virus infection (Hallak et al., 2000). The results from the

Table 3
ID_{50} of heparin against infection of MLVs into NIH 3T3 cells in the presence or absence of polybrene.

Polybrene	Viruses		
	F	A8	PVC-211
Present	44.4 ± 6.7	47.9 ± 0.8	49.6 ± 2.2
Absent	0.56 ± 0.08[a]	0.61 ± 0.10[a]	0.60 ± 0.05[a]

ID_{50} values (μg/ml) were calculated from the data shown in Fig. 5. The mean values (and SEMs) of 4 independent experiments are shown. Statistical comparison was performed using the t test.

[a] $P < 0.001$ vs presence of polybrene in each virus.

Position	Amino Acid F	A8	PVC-211	Structural element
-28	Pro	Ser	Ser	
1	Ala	Val	Ala	RBD
40	Val	Asp	Asp	RBD
61	Gln	Arg	Arg	RBD-VRA
79	Ser	Asn	Asn	RBD-VRA
80	Ser	Arg	Arg	RBD-VRA
84	Ser	Ser	Ala	RBD-VRA
116	Glu	Gly	Gly	RBD-VRA
129	Glu	Glu	Lys	RBD-VRC
152	Val	Ala	Ala	RBD
172	Ser	Asn	Asn	RBD-VRB
175	Val	Ala	Ala	RBD-VRB
203	Thr	Ile	Ile	RBD
216	Arg	Gln	Gln	RBD
227	Arg	Lys	Lys	RBD
249	Leu	Phe	Phe	
251	Arg	Leu	Leu	
263	Pro	Ser	Ser	
277	Thr	Ala	Ala	
319	Gly	Ala	Ala	
344	Val	Ala	Ala	
345	Ala	Gly	Gly	
358	Arg	Gln	Gln	
379	Ile	Thr	Thr	
380	Asp	Gly	Gly	
390	Thr	Ala	Ala	
393	Thr	Met	Met	
642	End	Gln	Gln	

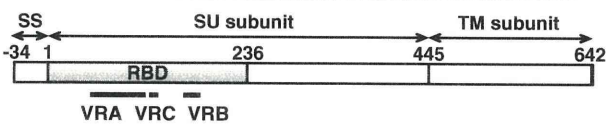

Fig. 6. Amino acid sequences of F-, A8-, and PVC-211-Env. A schematic diagram of the Env precursor polyprotein is shown at the bottom. SS: signal sequence; SU: surface protein; TM: transmembrane protein; RBD: receptor-binding domain (Fass et al., 1997); VRA: variable region A; VRB: variable region B; VRC: variable region C. The N-terminal amino acid of the SU is numbered as 1.

earlier studies and from here suggest that different types of sulfate groups are required for the inhibitory activities of heparin against different viruses, and that the anti-viral activity of heparin does not depend simply on negative charge density but involves particular structures, notably sulfation patterns.

Although the interaction between Env and CAT-1, the receptor molecule for MLV, appears to be required for membrane fusion and entry of the viral capsid, it has been reported that initial attachment of MLV to the cell surface can take place in a receptor-independent manner (Guibinga et al., 2002; Pizzato et al., 1999; Walker et al., 2002). Heparan sulfate on the cell surface was proposed as a candidate cell surface molecule for MLV attachment (Batra et al., 1997; Guibinga et al., 2002; Jinno-Oue et al., 2001; Le Doux et al., 1996, 1999; Masuda et al., 1997; Walker et al., 2002). The SPR analyses carried out in the present study also suggest that heparan sulfate on the cell surface is involved in MLV attachment as we found that heparin could bind directly to the Env of MLV. The exact role(s) of the cell surface heparan sulfate in MLV infection is still unknown; nevertheless,

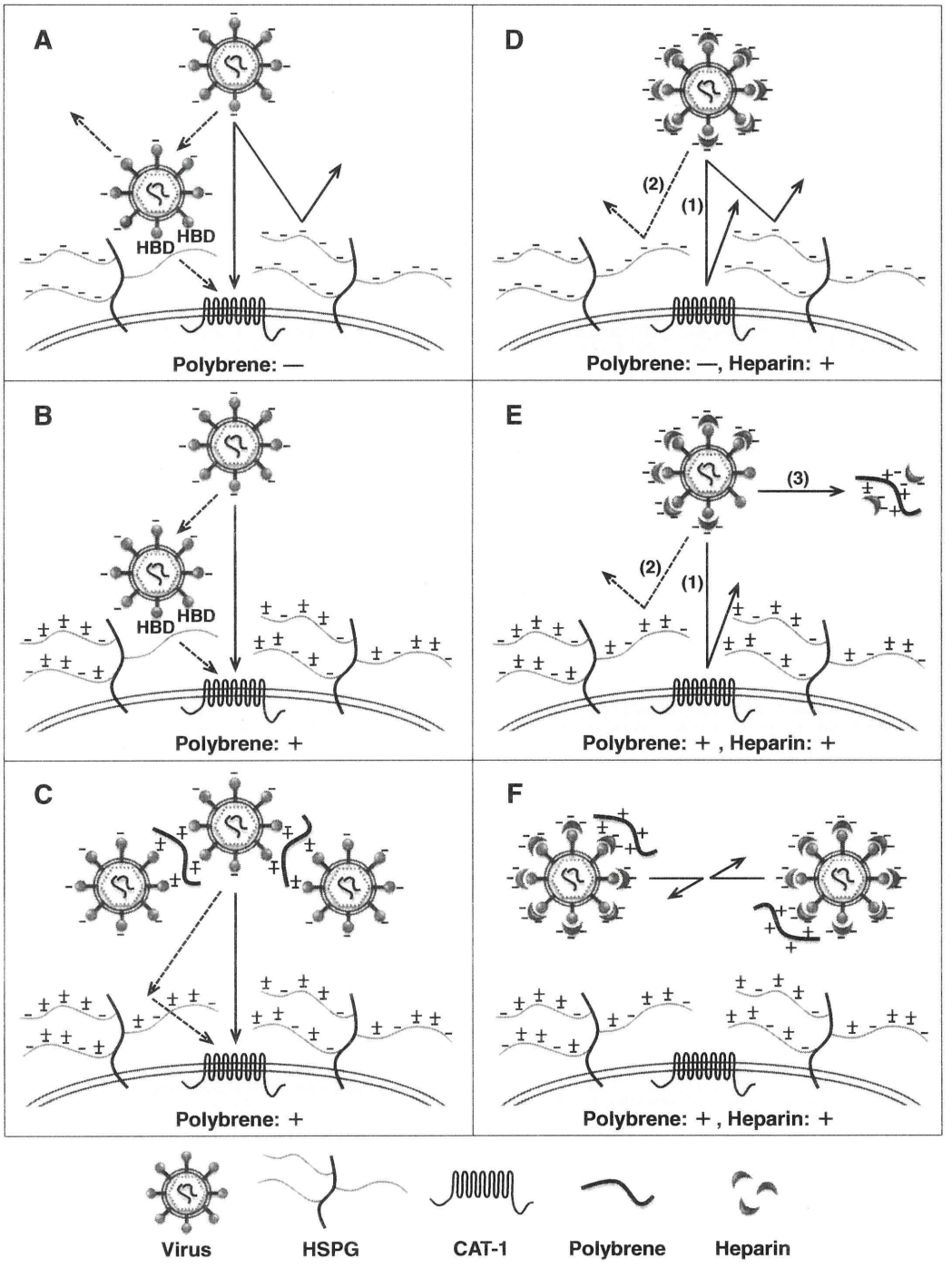

Fig. 7. Schematic diagrams of possible mechanisms of attachment of MLV to cells and of the inhibition of attachment by heparin. These various possibilities are described in detail in the Discussion section. CAT-1: cationic amino acid transporter 1 as the specific receptor for ecotropic MLV; HSPG: heparan sulfate proteoglycan.

we suggest a possible model for its behavior in Fig. 7. In this model, heparan sulfate on the cell surface is envisaged as a route for viral infection. The viral particles first bind to heparan sulfate via the HBD of Env and the increase in concentration of viral particles on the cell surface then raises the probability of interaction with CAT-1. On the cell surface, CAT-1 is covered by long chains of heparan sulfate that have a large net negative charge. In the absence of polybrene, it is difficult for viral particles with a negative charge to approach CAT-1 and/or heparan sulfate on the cell surface due to electrostatic repulsion (Fig. 7A). MLV infections are usually carried out in the presence of cationic polymers, such as polybrene to enhance infection, because the infectivity of MLV is very low in the absence of polybrene (Davis et al., 2002). Polybrene appears to enhance the infectivity of MLVs through various possible mechanisms, and some of these have been identified in previous studies. Initially, the positive charge of polybrene might neutralize the negative charge on the cell surface, facilitating access of the viral particles to CAT-1 and/or heparan sulfate on the cell surface (Fig. 7B) (Davis et al., 2004). A second possibility is that polybrene might cause the viral particles to form aggregates that have easier access to the cell surface (Fig. 7C) (Davis et al., 2004; Landazuri and Le Doux, 2004). Based on these putative mechanisms, how might heparin inhibit infection by ecotropic MLV? It is possible that heparin binds to a region near the RBD of Env and sterically or electrostatically blocks interaction between Env and CAT-1 (arrow (1) in Figs. 7D and E). A second possibility is that heparin binds to HBD of Env and that viral particles covered with heparin cannot bind to heparan sulfate on the cell surface (arrow (2) in Figs. 7D and E). Alternatively, viral particles bearing heparin have a large net negative charge and might fail to access the cell surface due to electrostatic repulsion. A final possibility is that polybrene might not be able to aggregate heparin-covered viral particles that bear large negative charges, and this might make access to the cell surface less efficient (Fig. 7F). The ID_{50} values of heparin for F-, A8, and PVC-211 MLVs were lower in the absence of polybrene than in its presence (Fig. 5 and Table 3). In the absence of polybrene, the negative charge of cell surface molecules is not neutralized. Therefore, it is possible that the repulsion between viral particles bearing heparin and cell surface molecules with a negative charge is stronger in the absence of polybrene than in its presence (Figs. 7D and E). As a result, heparin is able to inhibit viral infection effectively in the absence of polybrene. Alternatively, in the presence of polybrene, the part of the heparin molecule that normally binds to viral particles might instead bind with polybrene (arrow (3) in Fig. 7E), with the consequence that a relatively large amount of heparin is required for inhibition of viral infection.

Materials and methods

Reagents

Heparin (H4784), *N*-acetylheparin (A8036) (NA-H), de-*N*-sulfated heparin (D4776) (dNS-H), and *N*-acetyl-de-*O*-sulfated heparin (A6039) (NAdOS-H) were obtained from Sigma. Heparin obtained from Nacalai Tesque was used in the SPR analysis.

Cells and viruses

NIH 3T3 cells were grown in Dulbecco's modified Eagle's medium (DMEM) containing 10% fetal calf serum (FCS). *Mus dunni* cells were grown in RPMI1640 medium containing 10% FCS. 293T cells were grown on DMEM containing 5% FCS.

Infectious DNA clones of neuropathogenic A8 (Takase-Yoden and Watanabe, 1997; Watanabe and Takase-Yoden, 1995) (database ID: D88386) and PVC-211 MLVs (Kai and Furuta, 1984; Masuda et al., 1992) (database ID: M93134.1) and non-neuropathogenic F-MLV clone 57 (Oliff et al., 1980) (database ID: X02794) were described previously. NIH 3T3 cells were transfected with each DNA clone, and culture supernatants of the virus-producing cells were harvested and stored at −80 °C as stock viruses. Virus titers were determined by a focal immunoassay on *Mus dunni* cells in the presence of 10 μg/ml polybrene as described previously (Czub et al., 1991).

Assay of viral reverse transcriptase

Culture supernatants of the virus-producing cells were centrifuged at 5000 rpm for 5 min at 4 °C. To disrupt the viral particles, 10 μl of the supernatant was mixed with 14 μl of an aqueous solution of 7 mM Tris–HCl (pH7.6), 70 mM NaCl, 0.7 mM ethylenediaminetetraacetic acid (EDTA), and 0.03% Triton X-100. The mixture was then mixed with 16 μl of an aqueous solution of 125 mM Tris–HCl (pH7.6), 150 mM NaCl, 25 mM dithiothreitol, 2.5 mM $MnCl_2$, 250 μg/ml Poly(A) x $(dT)_{15}$ (Roche Diagnostics), and ^{3}H-TTP (1 μCi), and incubated for 1 h at 37 °C (Robert-Guroff et al., 1977). The reaction was stopped by addition of 1 μl 0.5 M EDTA, and incorporated radioactivity was determined as described previously (Tamura and Takano, 1978).

VSV based-pseudotyped viruses

Recombinant VSV, VSVΔG*/GFP-G, was kindly provided by Dr. Whitt. The virus carries the jellyfish GFP gene in place of the viral G protein gene, and its G protein is supplemented by a separate expression vector (Takada et al., 1997). The *env* genes of F-, A8, and PVC-211 MLVs were each cloned into a pCAGGS expression vector (pCAGGS-F-env, pCAGGS-A8-env, and pCAGGS-PVC-211-env, respectively). pCAGGS was kindly provided by Dr. Miyazaki, and transfected into 293T cells. To prepare VSV-based pseudotyped viruses, the cells were infected 24 h after transfection with VSVΔG*/GFP-G at an MOI of 10. After 12 h, the supernatant of each culture was replaced with fresh medium, and the cells were cultured for an additional 12 h. The culture supernatants were then collected, passed through a 0.22 μm pore size filter and stored at −80 °C as VSV-based pseudotyped viruses: VSV/F-Env, VSV/A8-Env, and VSV/PVC-211-Env, carrying Env of F-, A8, and PVC-211 MLVs, respectively. 293T cells that had not been transfected with the Env expression vector were also infected with VSVΔG*/GFP-G for preparing VSV viruses-like particles lacking Env (VSV/ΔEnv). To measure viral titer, NIH 3T3 cells were infected with each of the pseudotyped viruses in the presence of 10 μg/ml of polybrene and, at 16 h post-infection, GFP-positive cells were counted by flow cytometry.

FACS analysis

Cells were harvested and washed twice with FACS buffer (phosphate-buffered saline [PBS] containing 0.25% FCS, 0.25% horse serum, and 0.1% sodium azide). Then, the cells were suspended in FACS buffer and analyzed for GFP expression using a FACSAria Cell Sorter (BD Biosciences).

Immunoblot analysis

Western blot analysis was performed on 293T cells transfected with pCAGGS-F-env, pCAGGS-A8-env, or pCAGGS-PVC-211-env vectors, or with virions of VSV/F-Env, VSV/A8-Env, VSV/PVC-211-Env, VSV/ΔEnv; Mock transfected cells were used as a control. Cells were harvested at 48 h after transfection with the *env* expression vector. Cells were washed with PBS and then lysed with 2% sodium dodecyl sulfate (SDS) and 0.5 mM phenylmethylsulfonyl fluoride (PMSF) in PBS at 100 °C for 5 min. Nucleic acid was mechanically sheared using a syringe with a 22-gauge needle. A 1 ml aliquot of each virus supernatant, containing the 2×10^5 infectious units, was then subjected to ultracentrifugation at 30,000 rpm in a Beckman SW 41 Ti

rotor at 4 °C for 2 h to purify the virions. Precipitates containing virions were suspended in PBS. Sample buffer (5×) containing SDS, DTT, glycerol, and bromophenol blue in Tris–HCl (pH 6.8) was added to the cell lysate or the virion suspension. After boiling for 5 min, the lysates were loaded on a 10% SDS-polyacrylamide gel and electrophoresed. The proteins were then transferred to an Immobilon P membrane (Millipore) by electroblotting. To detect the Env protein, goat anti-Rauscher MLV gp70 (Quality Biotech Incorporated-Resource Laboratory) was used. Actin was detected using rabbit anti-beta-actin (Santa Cruz Biotechnology) as a loading control. Horseradish peroxidase-conjugated anti-goat IgG antibody and horseradish peroxidase-conjugated anti-rabbit IgG antibody (Santa Cruz Biotechnology) were used as secondary antibodies. The membrane was developed with ECL plus reagents (GE Healthcare). Band images were captured with LAS-3000 (FUJIFILM).

Preparation of VSV based-pseudotyped viruses for SPR analysis

Suspensions of VSV/F-Env, VSV/A8-Env, or VSV/PVC-211-Env (1×10^6 infectious units) were made up to 5 ml by adding fresh culture medium; they were then dialyzed in a cellulose tube (EIDIA Co., Ltd.) against 200× PBS (v/v) for 24 h at 4 °C, with the outer solution refreshed four times. Then, the solutions were fixed with 2% paraformaldehyde (PFA) buffered with 0.12 M phosphate (pH7.3). To remove the PFA, the solutions were dialyzed in a cellulose tube against 200× PBS (v/v) for 24 h at 4 °C, with the outer solution refreshed four times. Then, the solutions were concentrated at 4 °C to 0.5 ml (2×10^6 infectious units/ml) using an Amicon Ultra-15 100 K Centrifugal Filter Device (Millipore) and stored at −80 °C until use. For the negative control, we used an aliquot of the culture supernatant of VSV/ΔEnv-producing 293T cells; for the Mock control, we used an aliquot of the culture supernatant of 293T cells. For both controls, the aliquot was equivalent in volume to the sample from the culture supernatant of VSV/Env-producing cells, which contained 1×10^6 infectious units, and was treated in the same manner as above.

SPR analysis

Heparin, NAdOS-H and dNS-H were dialyzed against distilled water using an MWCO3500 membrane (SpectroPore), lyophilized, and then conjugated with an f-mono linker molecule to prepare the ligand conjugate as previously described (Sato et al., 2009; Suda et al., 2006). To prepare the Sugar Chip with immobilized ligand, the surface of a gold-coated chip (SUDx-Biotec) was oxidatively washed with UV ozone cleaner (Structure Probe Inc.) for 20 min and then immersed in 1 μM of the ligand conjugate dissolved in 50% (v/v) methanol solution overnight at room temperature with gentle agitation. The Sugar Chip was washed sequentially with water, 0.05% Tween 20, and water and dried at room temperature. For the SPR analysis, the Sugar Chip was set on a prism with refraction oil (nD = 1.518, Cargill Laboratories Inc.) in an SPR apparatus (SPR670M, Moritex). The SPR measurements were performed at room temperature according to the manufacturer's instructions, using PBS containing 0.05% Tween 20 as the running buffer at a flow rate of 15 μl/min.

Acknowledgments

We thank Dr. M. A. Whitt for providing VSVΔG*/GFP-G, and Dr. J. Miyazaki for providing pCAGGS. This work was supported in part by funding from MEXT (Ministry of Education, Culture, Sports, Science and Technology), the Matching Fund for Private Universities, S0901015, 2009–2014.

References

Albritton, L.M., Tseng, L., Scadden, D., Cunningham, J.M., 1989. A putative murine ecotropic retrovirus receptor gene encodes a multiple membrane-spanning protein and confers susceptibility to virus infection. Cell 57, 659–666.

Batra, R.K., Olsen, J.C., Hoganson, D.K., Caterson, B., Boucher, R.C., 1997. Retroviral gene transfer is inhibited by chondroitin sulfate proteoglycans/glycosaminoglycans in malignant pleural effusions. J. Biol. Chem. 272, 11736–11743.

Capila, I., Linhardt, R.J., 2002. Heparin–protein interactions. Angew. Chem. 41, 391–412.

Cardin, A.D., Weintraub, H.J., 1989. Molecular modeling of protein–glycosaminoglycan interactions. Arteriosclerosis 9, 21–32.

Copeland, R., Balasubramaniam, A., Tiwari, V., Zhang, F., Bridges, A., Linhardt, R.J., Shukla, D., Liu, J., 2008. Using a 3-*O*-sulfated heparin octasaccharide to inhibit the entry of herpes simplex virus type 1. Biochemistry 47, 5774–5783.

Crublet, E., Andrieu, J.P., Vives, R.R., Lortat-Jacob, H., 2008. The HIV-1 envelope glycoprotein gp120 features four heparan sulfate binding domains, including the co-receptor binding site. J. Biol. Chem. 283, 15193–15200.

Czub, M., Czub, S., McAtee, F.J., Portis, J.L., 1991. Age-dependent resistance to murine retrovirus-induced spongiform neurodegeneration results from central nervous system-specific restriction of virus replication. J. Virol. 65, 2539–2544.

Davis, H.E., Morgan, J.R., Yarmush, M.L., 2002. Polybrene increases retrovirus gene transfer efficiency by enhancing receptor-independent virus adsorption on target cell membranes. Biophys. Chem. 97, 159–172.

Davis, H.E., Rosinski, M., Morgan, J.R., Yarmush, M.L., 2004. Charged polymers modulate retrovirus transduction via membrane charge neutralization and virus aggregation. Biophys. J. 86, 1234–1242.

Fass, D., Davey, R.A., Hamson, C.A., Kim, P.S., Cunningham, J.M., Berger, J.M., 1997. Structure of a murine leukemia virus receptor-binding glycoprotein at 2.0 angstrom resolution. Science 277, 1662–1666.

Guibinga, G.H., Miyanohara, A., Esko, J.D., Friedmann, T., 2002. Cell surface heparan sulfate is a receptor for attachment of envelope protein-free retrovirus-like particles and VSV-G pseudotyped MLV-derived retrovirus vectors to target cells. Mol. Ther. 5, 538–546.

Hallak, L.K., Spillmann, D., Collins, P.L., Peeples, M.E., 2000. Glycosaminoglycan sulfation requirements for respiratory syncytial virus infection. J. Virol. 74, 10508–10513.

Jinno-Oue, A., Oue, M., Ruscetti, S.K., 2001. A unique heparin-binding domain in the envelope protein of the neuropathogenic PVC-211 murine leukemia virus may contribute to its brain capillary endothelial cell tropism. J. Virol. 75, 12439–12445.

Kai, K., Furuta, T., 1984. Isolation of paralysis-inducing murine leukemia viruses from Friend virus passaged in rats. J. Virol. 50, 970–973.

Kim, J.W., Closs, E.I., Albritton, L.M., Cunningham, J.M., 1991. Transport of cationic amino acids by the mouse ecotropic retrovirus receptor. Nature 352, 725–728.

Krusat, T., Streckert, H.J., 1997. Heparin-dependent attachment of respiratory syncytial virus (RSV) to host cells. Arch. Virol. 142, 1247–1254.

Landazuri, N., Le Doux, J.M., 2004. Complexation of retroviruses with charged polymers enhances gene transfer by increasing the rate that viruses are delivered to cells. J. Gene Med. 6, 1304–1319.

Le Doux, J.M., Morgan, J.R., Snow, R.G., Yarmush, M.L., 1996. Proteoglycans secreted by packaging cell lines inhibit retrovirus infection. J. Virol. 70, 6468–6473.

Le Doux, J.M., Morgan, J.R., Yarmush, M.L., 1999. Differential inhibition of retrovirus transduction by proteoglycans and free glycosaminoglycans. Biotechnol. Prog. 15, 397–406.

Masuda, M., Remington, M.P., Hoffman, P.M., Ruscetti, S.K., 1992. Molecular characterization of a neuropathogenic and nonerythroleukemogenic variant of Friend murine leukemia virus PVC-211. J. Virol. 66, 2798–2806.

Masuda, M., Hanson, C.A., Dugger, N.V., Robbins, D.S., Wilt, S.G., Ruscetti, S.K., Hoffman, P.M., 1997. Capillary endothelial cell tropism of PVC-211 murine leukemia virus and its application for gene transduction. J. Virol. 71, 6168–6173.

Mondor, I., Ugolini, S., Sattentau, Q.J., 1998. Human immunodeficiency virus type 1 attachment to HeLa CD4 cells is CD4 independent and gp120 dependent and requires cell surface heparans. J. Virol. 72, 3623–3634.

Neyts, J., Snoeck, R., Schols, D., Balzarini, J., Esko, J.D., Van Schepdael, A., De Clercq, E., 1992. Sulfated polymers inhibit the interaction of human cytomegalovirus with cell surface heparan sulfate. Virology 189, 48–58.

Oliff, A.I., Hager, G.L., Chang, E.H., Scolnick, E.M., Chan, H.W., Lowy, D.R., 1980. Transfection of molecularly cloned Friend murine leukemia virus DNA yields a highly leukemogenic helper-independent type C virus. J. Virol. 33, 475–486.

Patel, M., Yanagishita, M., Roderiquez, G., Bou-Habib, D.C., Oravecz, T., Hascall, V.C., Norcross, M.A., 1993. Cell-surface heparan sulfate proteoglycan mediates HIV-1 infection of T-cell lines. AIDS Res. Hum. Retroviruses 9, 167–174.

Pizzato, M., Marlow, S.A., Blair, E.D., Takeuchi, Y., 1999. Initial binding of murine leukemia virus particles to cells does not require specific Env-receptor interaction. J. Virol. 73, 8599–8611.

Rider, C.C., Coombe, D.R., Harrop, H.A., Hounsell, E.F., Bauer, C., Feeney, J., Mulloy, B., Mahmood, N., Hay, A., Parish, C.R., 1994. Anti-HIV-1 activity of chemically modified heparins: correlation between binding to the V3 loop of gp120 and inhibition of cellular HIV-1 infection in vitro. Biochemistry 33, 6974–6980.

Robert-Guroff, M., Schrecker, A.W., Brinkman, B.J., Gallo, R.C., 1977. DNA polymerase gamma of human lymphoblasts. Biochemistry 16, 2866–2873.

Sato, M., Ito, Y., Arima, N., Baba, M., Sobel, M., Wakao, M., Suda, Y., 2009. High-sensitivity analysis of naturally occurring sugar chains, using a novel fluorescent linker molecule. J. Biochem. 146, 33–41.

Secchiero, P., Sun, D., De Vico, A.L., Crowley, R.W., Reitz Jr., M.S., Zauli, G., Lusso, P., Gallo, R.C., 1997. Role of the extracellular domain of human herpesvirus 7 glycoprotein B in virus binding to cell surface heparan sulfate proteoglycans. J. Virol. 71, 4571–4580.

Shukla, D., Liu, J., Blaiklock, P., Shworak, N.W., Bai, X., Esko, J.D., Cohen, G.H., Eisenberg, R.J., Rosenberg, R.D., Spear, P.G., 1999. A novel role for 3-O-sulfated heparan sulfate in herpes simplex virus 1 entry. Cell 99, 13–22.

Suda, Y., Arano, A., Fukui, Y., Koshida, S., Wakao, M., Nishimura, T., Kusumoto, S., Sobel, M., 2006. Immobilization and clustering of structurally defined oligosaccharides for sugar chips: an improved method for surface plasmon resonance analysis of protein–carbohydrate interactions. Bioconjug. Chem. 17, 1125–1135.

Takada, A., Robison, C., Goto, H., Sanchez, A., Murti, K.G., Whitt, M.A., Kawaoka, Y., 1997. A system for functional analysis of Ebola virus glycoprotein. Proc. Natl. Acad. Sci. U. S. A. 94, 14764–14769.

Takase-Yoden, S., Watanabe, R., 1997. Unique sequence and lesional tropism of a new variant of neuropathogenic Friend murine leukemia virus. Virology 233, 411–422.

Tamura, T.-A., Takano, T., 1978. A new, rapid procedure for the concentration of C-type viruses from large quantities of culture media: ultrafiltration by diaflo membrane and purification by ficoll gradient centrifugation. J. Gen. Virol. 41, 135–141.

Trybala, E., Bergström, T., Spillmann, D., Svennerholm, B., Olofsson, S., Flynn, S.J., Ryan, P., 1996. Mode of interaction between pseudorabies virus and heparan sulfate/heparin. Virology 218, 35–42.

Trybala, E., Liljeqvist, J.A., Svennerholm, B., Bergström, T., 2000. Herpes simplex virus types 1 and 2 differ in their interaction with heparan sulfate. J. Virol. 74, 9106–9114.

Walker, S.J., Pizzato, M., Takeuchi, Y., Devereux, S., 2002. Heparin binds to murine leukemia virus and inhibits Env-independent attachment and infection. J. Virol. 76, 6909–6918.

Wang, H., Kavanaugh, M.P., North, R.A., Kabat, D., 1991. Cell-surface receptor for ecotropic murine retroviruses is a basic amino-acid transporter. Nature 352, 729–731.

Watanabe, R., Takase-Yoden, S., 1995. Gene expression of neurotropic retrovirus in the CNS. Prog. Brain Res. 105, 255–262.

WuDunn, D., Spear, P.G., 1989. Initial interaction of herpes simplex virus with cells is binding to heparan sulfate. J. Virol. 63, 52–58.

Xia, G., Chen, J., Tiwari, V., Ju, W., Li, J.P., Malmstrom, A., Shukla, D., Liu, J., 2002. Heparan sulfate 3-O-sulfotransferase isoform 5 generates both an antithrombin-binding site and an entry receptor for herpes simplex virus, type 1. J. Biol. Chem. 277, 37912–37919.

Ye, S., Luo, Y., Lu, W., Jones, R.B., Linhardt, R.J., Capila, I., Toida, T., Kan, M., Pelletier, H., McKeehan, W.L., 2001. Structural basis for interaction of FGF-1, FGF-2, and FGF-7 with different heparan sulfate motifs. Biochemistry 40, 14429–14439.

CHEMISTRY
A EUROPEAN JOURNAL

DOI: 10.1002/chem.201003581

Chemical Synthesis of *Helicobacter pylori* Lipopolysaccharide Partial Structures and their Selective Proinflammatory Responses

Atsushi Shimoyama,[a] Akinori Saeki,[a] Natsuko Tanimura,[b] Hiroko Tsutsui,[c] Kensuke Miyake,[b] Yasuo Suda,[d] Yukari Fujimoto,*[a] and Koichi Fukase*[a]

Abstract: *Helicobacter pylori* is a common cause of gastroduodenal inflammatory diseases such as chronic gastritis and peptic ulcers and also an important factor in gastric carcinogenesis. Recent reports have demonstrated that bacterial inflammatory processes, such as stimulation with *H. pylori* lipopolysaccharide (LPS), initiate atherosclerosis. To establish the structures responsible for the inflammatory response of *H. pylori* LPS, we synthesized various kinds of lipid A structures (i.e., triacylated lipid A and Kdo-lipid A compounds), with or without the ethanolamine group at the 1-phosphate moiety, by a new divergent synthetic route. Stereoselective α-glycosylation of Kdo *N*-phenyltrifluoroacetimidate was achieved by use of microfluidic methods. None of the lipid A and Kdo-lipid A compounds were a strong inducer of IL-1β, IL-6, or IL-8, suggesting that *H. pylori* LPS is unable to induce acute inflammation. In fact, the lipid A and Kdo-lipid A compounds showed antagonistic activity against cytokine induction by *E. coli* LPS, except for the lipid A compound with the ethanolamine group, which showed very weak agonistic activity. On the other hand, these *H. pylori* LPS partial structures showed potent IL-18- and IL-12-inducing activities. IL-18 has been shown to correlate with chronic inflammation, so *H. pylori* LPS might be implicated in the chronic inflammatory responses induced by *H. pylori*. These results also indicated that *H. pylori* LPS can modulate the immune response: NF-κB activation through hTLR4/MD-2 was suppressed, whereas production of IL-18 and IL-12 was promoted.

Keywords: glycolipids · glycosylation · inflammation · immunochemistry · synthetic methods

Introduction

Helicobacter pylori is one of the Gram-negative bacteria, and its chronic colonization of the human stomach is the major risk factor for gastroduodenal inflammatory diseases such as chronic gastritis and peptic ulcers and also contributes to gastric carcinogenesis.[1,2] The prevalence of *H. pylori* infections is estimated to be half of the world population. Although the majority of infections are asymptomatic, approximately 10–20% of infected people will develop peptic ulcers, and 1% will develop gastric cancer.[3] Lipopolysaccharide (LPS) of Gram-negative bacteria, also called endotoxin, is generally a potent immunostimulator and can cause sepsis during severe infection. However, the *H. pylori* LPS shows very low toxic activity in comparison with other enterobacterial preparations, such as *Escherichia coli* LPS, and seems instead to be a key factor in virulence expression and the innate immune response to infection.[4–7] In fact, the plague bacillus *Yersinia pestis* produces LPS with poor stimulating activity for Toll-like receptor 4 (TLR4) to evade LPS-induced inflammation and to establish a deadly infection.[8]

It was recently reported that chronic infections are associated with atherosclerosis, which is a chronic inflammatory vascular disease[9–11] and a major factor in cardiovascular disease, a primary cause of death worldwide. The inflammatory process in atherosclerosis is thought to be initiated by infectious agents such as *H. pylori*,[10,11] *Chlamydia pneumoniae*,[12–14] or *Porphyromonas gingivalis*.[15–18] In particular, LPS has been implicated in atherosclerosis,[14–16,18] and Triantafilou et al. showed that LPS from *H. pylori* and *P. gingivalis* induces inflammatory responses in human vascular endothelial cells.[19] Several recent reports also suggested a linkage between neuropathological conditions in the central nervous system (CNS), such as Alzheimer's disease, and infectious agents including some viruses and bacteria (e.g.,

[a] Dr. A. Shimoyama, A. Saeki, Prof. Y. Fujimoto, Prof. K. Fukase
Department of Chemistry, Graduate School of Science
Osaka University, Toyonaka, Osaka 560-0043 (Japan)
Fax: (+81) 6-6850-5419
E-mail: yukarif@chem.sci.osaka-u.ac.jp

[b] Dr. N. Tanimura, Prof. K. Miyake
Division of Infectious Genetics
Institute of Medical Science, The University of Tokyo
4-6-1 Shirokanedai, Minatoku Tokyo 108-8639 (Japan)

[c] Prof. H. Tsutsui
Department of Microbiology, Hyogo College of Medicine
1-1, Mukogawa, Nishinomiya, Hyogo 663-8501 (Japan)

[d] Prof. Y. Suda
Department of Chemistry, Biotechnology and Chemical Engineering
Graduate School of Science and Engineering, Kagoshima University
Kagoshima 890-0065 (Japan)

Supporting information for this article is available on the WWW under http://dx.doi.org/10.1002/chem.201003581.

H. pylori, *C. pneumoniae*, and spirochete).[20] Proinflammatory cytokines, particularly interleukin 18 (IL-18),[21] are thought to be related to chronic inflammatory diseases such as atherosclerosis[22] and to neuroinflammatory/neurodegenerative processes in the CNS.[23] Although various studies have shown a correlation between up-regulation of IL-18 and *H. pylori* infection,[24–26] the substances responsible for IL-18 production have not been well elucidated, except in Suda's report,[27] which indicated that *H. pylori* LPS induces IL-18. We hence synthesized various lipid A partial structures in order to investigate the immunoregulatory effects of *H. pylori* lipid A and LPS and to establish the structures responsible for the inflammatory response.

The endotoxic activity of LPS originates from lipid A, a glycolipid terminal structure of LPS. In general, lipid A is composed of two glucosamine (GlcN) units and fatty acids linked to the 2- and 2′-amino and 3- and/or 3′-hydroxy groups (Scheme 1, below). In the series of our synthetic studies of lipid A,[28–30] we found that lipid A compounds with smaller numbers of acyl groups (tri- and tetraacylated with saturated fatty acids, for example) showed antagonistic activity (against cytokine induction by *E. coli* LPS), whereas the *E. coli*-type hexaacylated lipid A showed potent immunostimulating activity. We observed that the presence of a Kdo residue along with lipid A enhances the activities.[31]

The lipid A moieties of parasitic bacteria (e.g., *H. pylori* and *P. gingivalis*) have characteristic structures, generally containing fewer but longer fatty acids than those of enterobacteria such as *E. coli* and frequently lacking one of the two phosphates. In fact, the characteristics of *H. pylori* lipid A are as follows: 1) it has fewer (tri- and tetraacylation are mostly found) but longer fatty acid residues (mainly C18), 2) the 4′-phosphate group is often absent, and 3) an ethanolamine group is often linked to the glycosyl phosphate moiety.[32,33] Detailed structural characterizations of the lipid A components of *H. pylori* were performed independently on the 206-1 strain by Suda et al.[32] and on the NCTC 11637 strain by Moran et al.[33] The *H. pylori* 206-1 strain mainly produced a triacyl-type lipid A, whereas the NCTC 11637 strain mainly produced the tetraacyl-type lipid A in rough and smooth LPS (R- and S-LPS) and the hexaacyl-type in the S-LPS as a minor component.

The LPS and lipid A preparations from *H. pylori* are heterogeneous and could be contaminated by other immunostimulants, so chemically synthesized pure compounds were required for precise biological studies. We have therefore previously synthesized the *H. pylori* lipid A structures triacyl-type *H. pylori* lipid A (**HpLA**, **1**, Scheme 1, below), triacyl-type *H. pylori* lipid A aminoethanol phosphate (**HpLAEA**, **2**), and *H. pylori* Kdo-lipid A (**HpKdoLA**, **3**).[27,31,34] **HpLAEA** (**2**), which contains an ethanolamine residue, induced lower levels of cytokines, such as IL-8 and TNF-α, upon activation of the LPS receptor, a Toll-like receptor 4 (TLR4)/MD-2 complex. In contrast, compounds **1** and **3** showed antagonistic activity against stimulation by *E. coli* LPS. **HpKdoLA** (**3**) showed more potent inhibitory activity than **HpLA** (**1**). A requirement for chemically synthesized pure compounds is also the case for *P. gingivalis* lipid A, and some synthetic works have also previously been done[35–37] for analysis of the immunostimulatory activities.

In this study we also synthesized a compound of the *H. pylori* Kdo-lipid A aminoethanol phosphate type (**HpKdoLAEA**, **4**) for the first time, as well as resynthesizing compounds **1**–**3** to elucidate their biological functions in detail. We developed a new divergent strategy, in which the key intermediate **9** (Scheme 1, below) was used as a common precursor for the various lipid A and Kdo-lipid A structures of *H. pylori*, *P. gingivalis*, and others. The divergent strategy was also employed in our previous synthesis and in Boons' synthesis.[38,39] Boons et al. synthesized Kdo-lipid A of *Neisseria meningitides* by a divergent strategy with use of a different synthetic intermediate.[40] Glycosylation of the lipid A part with the Kdo donor was difficult to accomplish, because considerable amounts of the glycal were formed as a by-product. We found that glycosylation with the Kdo donor **6** under microfluidic conditions effectively suppressed the glycal formation. The details of the synthetic strategy and the biological activities of compounds **1**–**4** are discussed below.

Results

The new diversity-oriented synthetic strategy for *H. pylori* lipid A/Kdo-lipid A compounds is illustrated in Scheme 1. The appropriately protected disaccharide **9** was synthesized as a common key intermediate from the monosaccharide donor **7** and the acceptor **8**. Each protecting group in **9** (i.e., 1-*O*-allyl, 2-*N*-allyloxycarbony (Alloc), 2′-*N*-2,2,2-trichloroethyloxycarbonyl (Troc), 3-*O*-benzyloxycarbonyl (Z), 3′-*O*-*p*-methoxybenzyl (MPM), and 4′,6′-benzylidene) could be selectively removed to enable sequential introduction variously of the Kdo moiety, acyl groups, or phosphate groups at the appropriate position. We also developed the new Kdo *N*-phenyltrifluoroacetimidate donor **6**, which can be activated by catalytic quantities of a Lewis acid. The acid-labile MPM group was hence utilizable as a temporary protective group in the lipid A part.

As shown in Scheme 2, the lipid A moieties were synthesized with and without the ethanolamine component at the 1-phosphate (compounds **1** and **2**). The glycosyl donor **7** and the acceptor **8** were synthesized independently from D-glucosamine hydrochloride in six steps (Schemes S1 and S2 in the Supporting Information). The donor **7** was synthesized via allyl 4,6-*O*-benzylidene-GlcNTroc,[38] with introduction of MPM and subsequent allyl group cleavage and introduction of trichloroacetoimidate at the anomeric position. The acceptor **8** was prepared via allyl 4,6-*O*-benzylidene-GlcNAlloc,[41] with introduction of MPM and selective opening of the benzylidene group to liberate the 6-hydroxy group, followed by cleavage of the MPM group. Glycosylation between the donor **7** and the acceptor **8** afforded the disaccharide with complete β-selectivity, owing to the neighboring effect of the Troc group of **7**, and the 3-position in

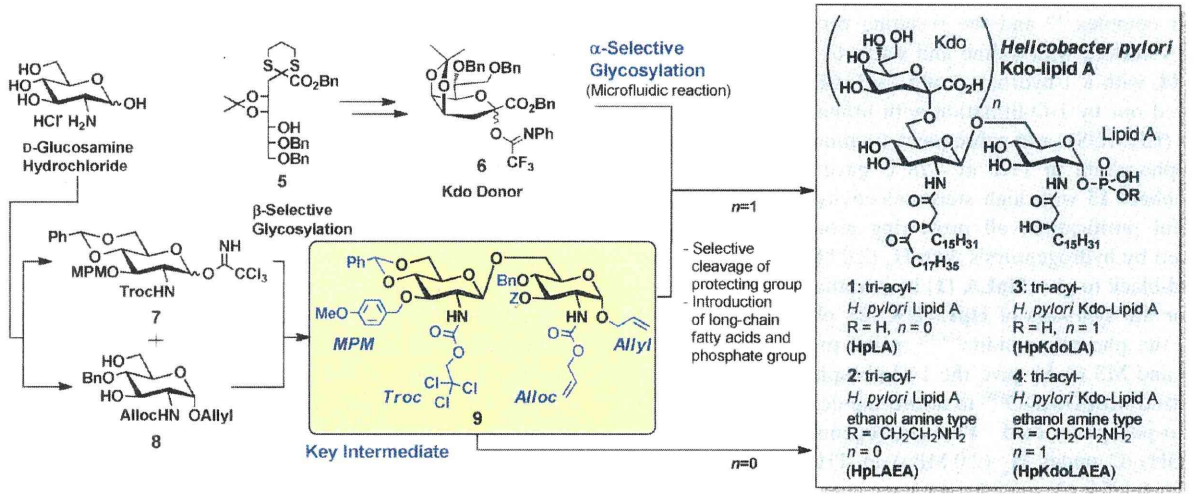

Scheme 1. Synthetic strategy for the triacyl-type *Helicobacter pylori* lipid A and Kdo-lipid A.

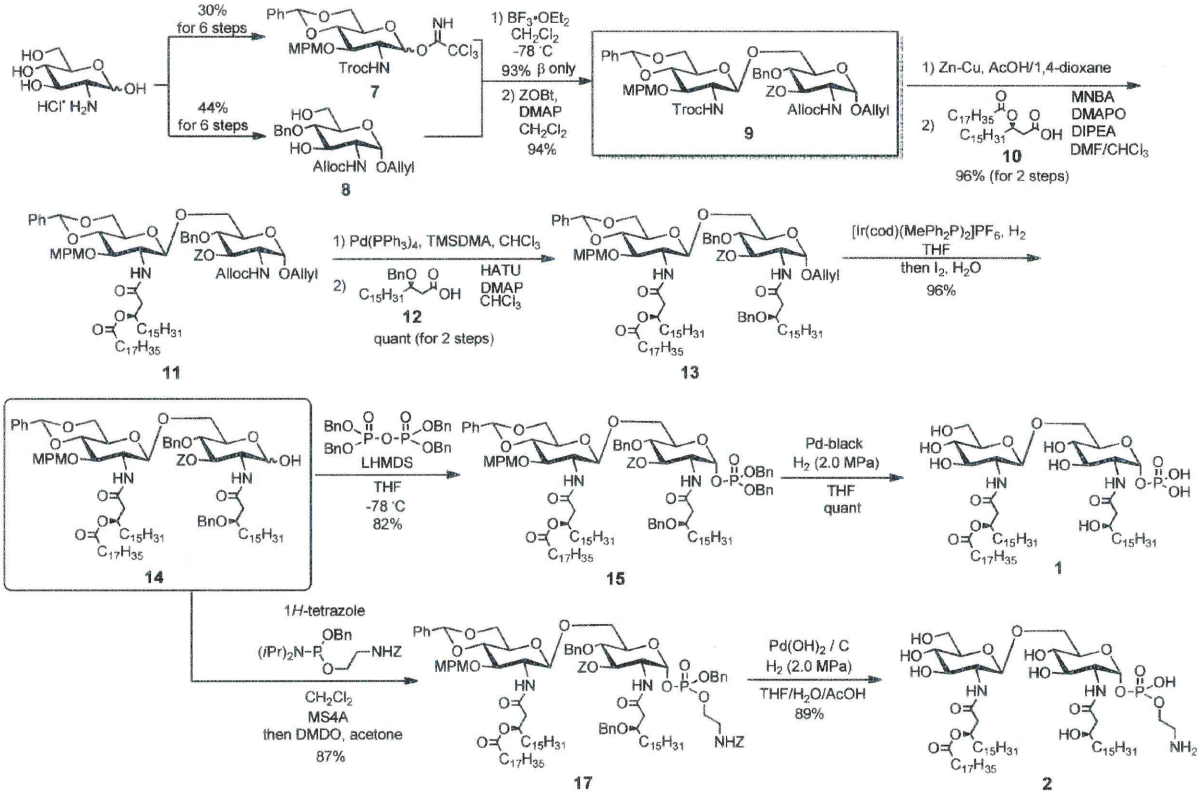

Scheme 2. The synthesis of the *Helicobacter pylori* lipid A compounds **1** and **2**.

the disaccharide was protected with a Z group to give the key intermediate **9**. The 2′-*N*-Troc group was then removed through the action of a Zn/Cu couple and acetic acid and the amino group was acylated with the acyloxycarboxylic acid **10** (Scheme S3 in the Supporting Information) by Shiina's method.[42] Other coupling methods gave considerable amounts of the symmetrical acid anhydride of **10**, which showed low reactivity in acylation here. Subsequently, the 2-*N*-Alloc group of **11** was removed by treatment with Pd-$(PPh_3)_4$ and dimethylaminotrimethylsilane (TMSDMA),[43] and the free 2-amino group was smoothly acylated with the benzyloxycarboxylic acid **12** (Scheme S3 in the Supporting Information) with use of *O*-(7-azabenzotriazol-1-yl)-*N,N,N′,N′*-tetramethyluronium hexafluorophosphate (HATU) and 4-(dimethylamino)pyridine (DMAP) to give the protected lipid A backbone **13** in quantitative yield. The

allyl group was then isomerized to a prop-1-enyl group with an Ir complex,[44] and the resulting prop-1-enyl group was then removed with iodine and water to yield the disaccharide **14**, with a 1-hydroxy group. 1-*O*-α-Phosphorylation was carried out by 1-*O*-lithiation with lithium hexamethyldisilazide (LHMDS), and subsequent treatment with tetrabenzyl pyrophosphate in THF at −78°C gave the desired 1-*O*-α-phosphate **15** with high stereoselectivity.[45] After rapid but careful purification, all protecting groups of **15** were removed by hydrogenolysis with H_2 (2.0 MPa) in the presence of Pd-black to give **HpLA (1)** in quantitative yield.

For the synthesis of **HpLAEA (2)**, phosphitylation of **14** with the phosphoramidite[46,47] in the presence of 1*H*-tetrazole and MS (4 Å) gave the 1-*O*-phosphite, which was then oxidized with DMDO[48] to afford the desired fully protected 1-*O*-α-phosphorylated **17**. Hydrogenolysis of **17** with $Pd(OH)_2/C$ under H_2 (2.0 MPa) in THF/H_2O/AcOH gave the **HpLAEA (2)** in 89% yield.

The polysaccharide component of LPS is linked to lipid A through a unique acidic octose: 3-deoxy-D-manno-2-octulosonic acid (Kdo). In our previous synthetic study of *E. coli* Re LPS compounds composed of lipid A and two Kdo residues, we showed that Kdo moieties enhanced the immunostimulating activity of lipid A.[49] On the other hand, **HpKdoLA (3)** showed stronger antagonistic activity than the lipid A part (**HpLA**, **1**).[31] Lipid A parts have previously been considered to represent the activity of LPS, but our studies showed that the effect of the Kdo varies depending on the LPS species. We hence synthesized **HpKdoLAEA (4)** to investigate the effect of the Kdo residue on the lipid A part in this study. Our group has developed α-selective glycosylation through the use of Kdo fluorides with bulky protecting groups such as isopropylidene and TBS groups at the 4- and 5-positions, and applied this to the synthesis of *E. coli* Re-type LPS.[49] With these Kdo donors, the undesirable β-side attack by a glycosyl acceptor is prevented by the presence of the bulky protective groups. Glycosylation with Kdo fluorides, however, requires a large excess of Lewis acid for the activation,[49] which has occasionally caused cleavage of the acid-labile TBS or isopropylidene groups and hence decreased the stereoselectivity in the glycosylation. The synthetic strategy was also constrained by the limited number of protective groups resistant to strongly acidic conditions. In this study, we therefore devised the new Kdo donors **6** and **18**, possessing *N*-phenytrifluoroacetimidate moieties. Glycosyl *N*-phenytrifluoroacetimidates have been shown to be very efficient donors, which can be activated by catalytic amounts of Lewis acid under mild conditions.[50] The Kdo donors **6** and **18** were synthesized from the intermediate **5** (Scheme 1), which was prepared from D-mannose by our reported methods (Scheme S4 in the Supporting Information).[49] The glycosyl disaccharide acceptor **19** was prepared by regioselective reductive ring-opening of the 4′,6′-*O*-benzylidene group in **9** with $Me_2NH{\cdot}BH_3$ and $BF_3{\cdot}OEt_2$ (Scheme 3A).

We first attempted the glycosylation of the Kdo donors **6** and **18** with the acylated disaccharide intermediates as the glycosyl acceptors, but the reactions did not proceed. Instead, the glycals were formed as by-products with intramolecular β-hydrogen elimination. We then examined glycosylation with the disaccharide acceptor **19**, which showed better reactivity than the acylated disaccharide intermediates. The glycosylation was carried out at 0°C with the isopropylidene Kdo donor **6** in excess (5 equiv) relative to **19** in the presence of TBSOTf (0.5 equiv) as a catalyst to give the desired trisaccharide **20** in 70% yield with high α-selectivity (Scheme 3B). The α-promoting solvent effect of cyclopentyl methyl ether (CPME) was employed here.[51,52] The trisaccharide **20** was thus obtained, although a large amount of the glycal was formed. On the other hand, glycosylation of **19** with the Kdo donor **18** did not occur at all. The lower reactivity of 4,5-*O*-TBS Kdo fluoride relative to the corresponding 4,5-*O*-isopropylidene was also observed in our previous study.[49]

Although the yield and stereoselectivity of the newly developed Kdo glycosylation were acceptable, a large excess of the glycosyl donor **6** was required for completion of the reaction. The low efficiency in the glycosylation might be due to difficulties in temperature control under the conventional batch reaction conditions, because the donor **6** was highly reactive and would be expected to generate a significant amount of heat during the reaction. We had previously reported α-selective sialylation with *N*-phenyltrifluoroacetimidate donors by use of a continuous flow microreactor, which enables efficient mixing and fast heat transfer, to increase the stereoselectivity and to suppress glycal formation.[53] We thus applied microfluidic glycosylation of the Kdo donor **6**, expecting suppression of the glycal formation owing to efficient removal of heat of reaction as well as the promotion of intermolecular coupling reaction because of efficient mixing (Scheme 3C). For this microfluidic Kdo glycosylation, a CPME solution of the Kdo donor **6** and the acceptor **19** was mixed with TBSOTf solution in CPME at various concentrations in an IMM microreactor at a flow rate of 0.5 mL min^{-1}. The reaction mixture was allowed to flow for an additional 42 seconds through a tubular reactor (Φ = 1.0 mm) and then quenched by addition to a saturated aqueous solution of sodium bicarbonate. After the optimization as shown in Scheme 3, the desired compound **20** was obtained in 72% yield with high stereoselectivity through mixing of a solution of the donor **6** (0.15 M) and the acceptor **19** (0.10 M) in CPME with a solution of TBSOTf (0.10 M) in CPME. Although the yield of microfluidic glycosylation was almost the same as that of the batch glycosylation, the formation of glycal was suppressed and only 1.5 equivalents of Kdo donor **6** relative to **19** were necessary for the microfluidic glycosylation. The rapid reaction achieved by the use of relatively higher concentrations of the Lewis acid led to the success of this microfluidic Kdo glycosylation without cleavage of the protecting groups.

The synthesis of the desired Kdo-lipid A compounds **3** and **4** from the trisaccharide **20** is shown in Scheme 4. The 2′-*N*-Troc group of **20** was removed with a Zn/Cu couple and the resulting amino group was acylated with the acyl-

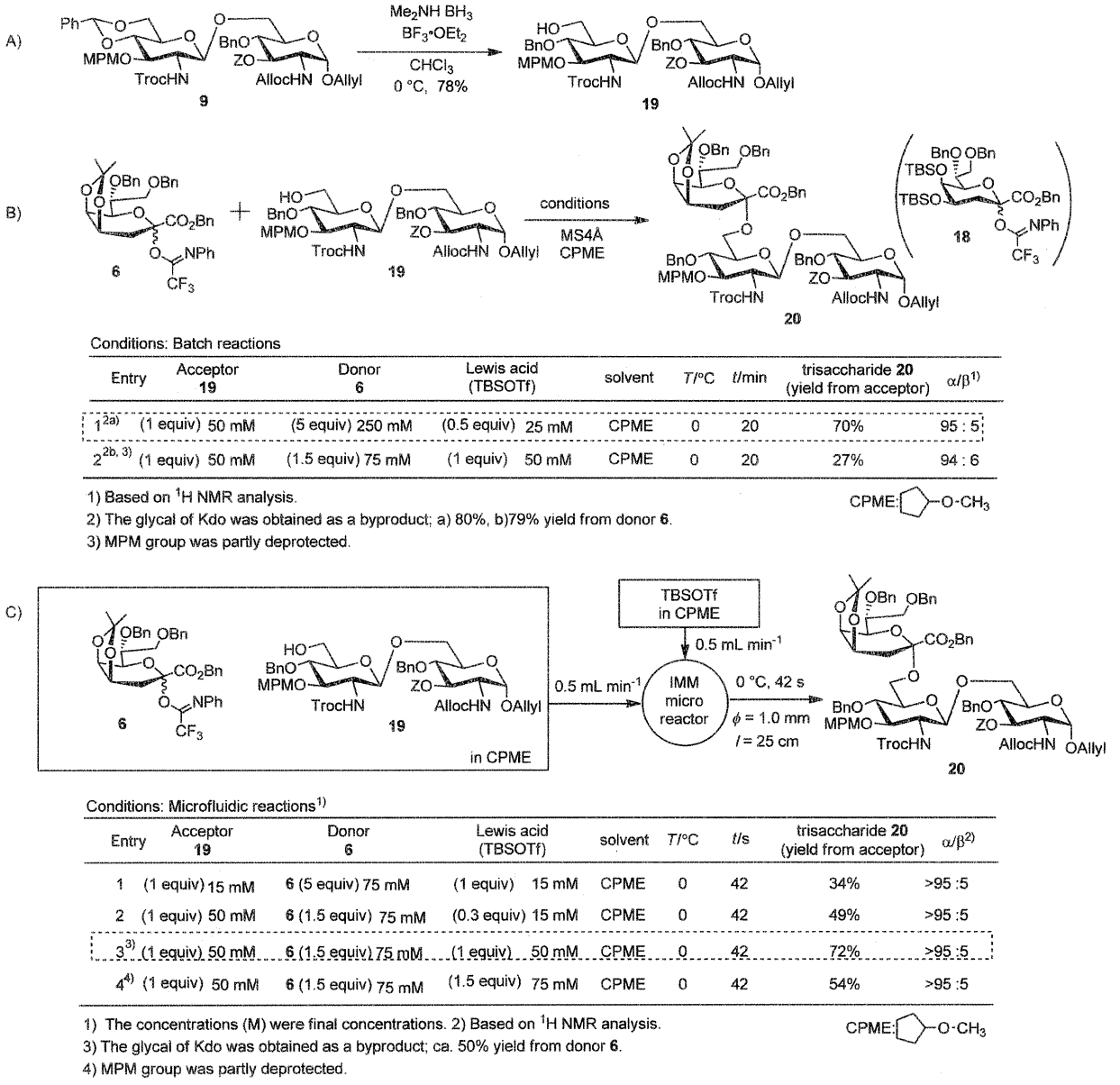

Scheme 3. The synthesis of Kdo-lipid A. A) The preparation of the disaccharide **19**. B), C) The α-selective glycosylation of Kdo B) by the conventional batch method, and C) by the microfluidic method.

oxycarboxylic acid **10** in the presence of 2-methyl-6-nitrobenzoic anhydride (MNBA) and *N,N*-diisopropylethylamine (DIPEA). For the acylation at this 2′-position, we also examined conditions with HATU, DMAP, and Et_3N, but these required more fatty acid and longer reaction times to finish the reaction, although the yield was much the same. The 2-*N*-Alloc group was then selectively cleaved by treatment with $Pd(PPh_3)_4$ and TMSDMA, and the liberated amino group was acylated with the benzyloxycarboxylic acid **12** in the presence of HATU and Et_3N to give the acylated trisaccharide **21** in an excellent yield (92%). For the synthesis of the **HpKdoLA** (**3**), the isopropylidene and 1-*O*-allyl groups in **21** were removed to yield **22**. The anomeric position in **22** was selectively phosphorylated with tetrabenzyl pyrophosphate and LHMDS, and all protecting groups were then removed by hydrogenolysis (H_2, 20 MPa) in the presence of Pd-black to afford the desired **HpKdoLA 3** in quantitative yield.

HpKdoLAEA (**4**) was synthesized by use of the phosphoroamidite method for 1-*O*-phosphorylation, as in the synthesis of **2**. Because of the high reactivity of the phosphoroamidite reagent it was necessary to protect all of the hydroxy groups except for the target 1-OH group for the phsphorylation step. The isopropylidene group in **21** was

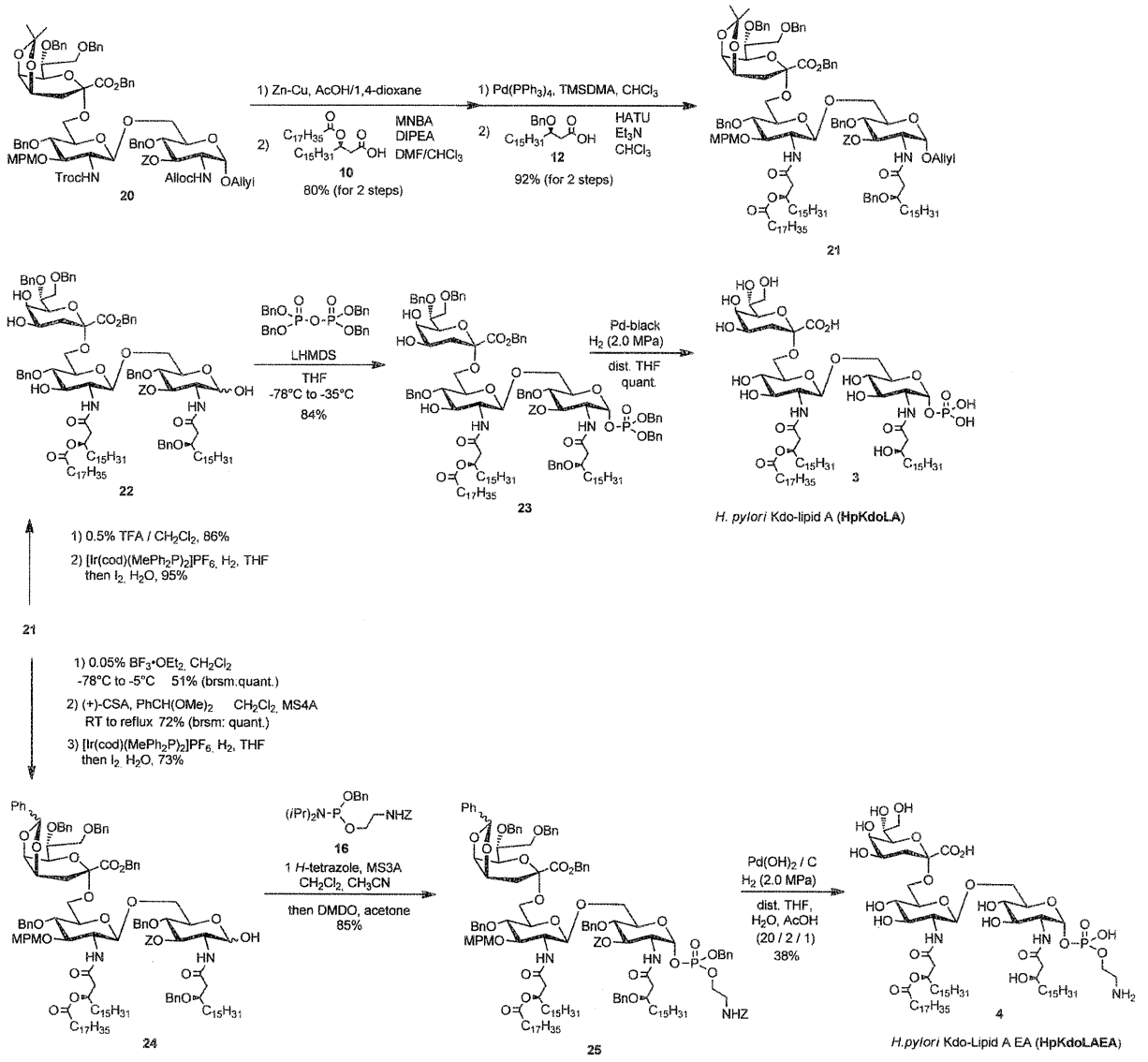

Scheme 4. The synthesis of the *Helicobacter pylori* Kdo-lipid A compounds **3** and **4**.

converted into a benzylidene group for the final deprotection by catalytic hydrogenolysis. The allyl group of the benzylidenated trisaccharide was cleaved to give the 1-*O*-free compound **24**. Phosphitylation of **24** was carried out with the phosphoramidite, the resulting phosphite was oxidized with dimethyldioxirane (DMDO), and all protecting groups were then removed by hydrogenolysis with $Pd(OH)_2/C$ in $THF/H_2O/AcOH$ under H_2 (2.0 MPa) to give the **HpKdoLAEA (4)**.

The immunomodulating activities of the synthesized *H. pylori* lipid A and Kdo-lipid A compounds were evaluated by induction or suppression of cytokines such as IL-1β, IL-6, IL-8, and IL-18 (Figure 1), as well as IL-12 and TNF-α (Figure S1 in the Supporting Information), relative to the *E. coli* LPS strain O111:B4. The cytokine-inducing activities were tested in human peripheral whole blood cells.[54] A mixture of a test sample and heparinized human peripheral whole blood was incubated at 37 °C for 20 h. The cytokine levels in the supernatants of the incubated mixtures were measured by an enzyme-linked immunosorbent assay (ELISA). Inhibitory activities were measured according to the abilities of the compounds to inhibit LPS-induced cytokine production as follows: the prepared samples, LPS (*E. coli* O111:B4, 500 pg mL^{-1}), and heparinized human peripheral whole blood were mixed and incubated, and the cytokine levels were measured. Because of the lower solubilities of the synthesized *H. pylori* lipid A and Kdo-lipid A compounds, concentrations higher than those in Figure 1 were not tested. Only the **HpLAEA** showed weak inducing activities of IL-1β, IL-6, IL-8, and TNF-α, whereas **HpLA**,

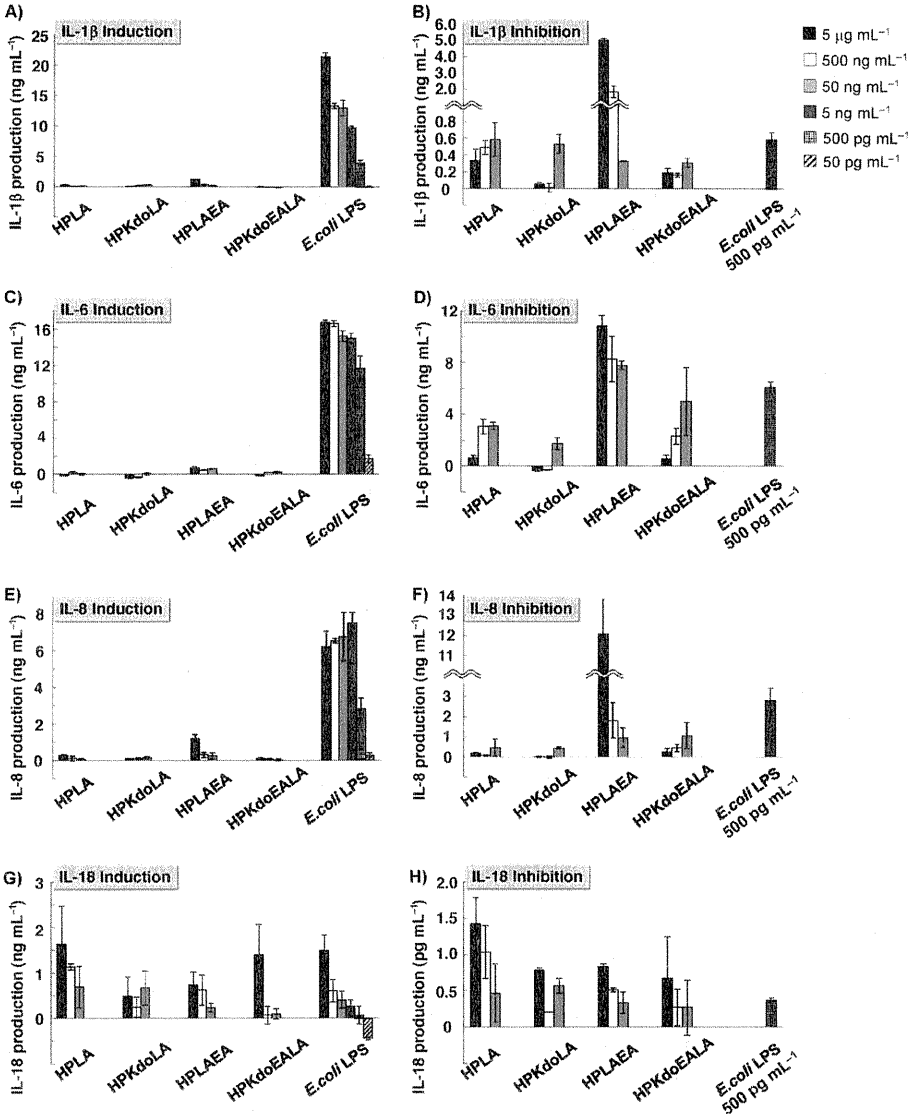

Figure 1. Cytokine induction and inhibition by the synthesized *H. pylori* triacyl-type lipid A compounds **1** (**HpLA**) and **2** (**HpLAEA**) and by the Kdo-lipid A compounds **3** (**HpKdoLA**) and **4** (**HpKdoLAEA**), relative to *E. coli* LPS O111:B4. Human peripheral whole-blood cells were assayed. A) Induction and B) inhibitory activities of IL-1β. C) Induction and D) inhibitory activities of IL-6. E) Induction and F) inhibitory activities of IL-8. G) Induction and H) inhibitory activities of IL-18. In the inhibitory assay, the *E. coli* LPS coexisted in the samples during the incubation at a concentration of 500 pg ml^{-1}.

HpKdoLA, and **HpKdoLAEA** showed not inducing activities but inhibitory activities toward cytokine induction by *E. coli* LPS (Figure 1A–F, Figure S1 A–C in the Supporting Information). **HpKdoLA** showed stronger inhibitory activities than **HpLA**, as we had previously reported. In the case of the aminoethanol phosphate-type lipid A compounds, the Kdo residue changed the activity of lipid A. Synergic enhancements of cytokine production with **HpLAEA** in combination with *E. coli* LPS were also observed (Figure 1B, 1D, and 1F). In the case of **HpLA**, synergic enhancement was also observed in the IL-6 inhibition assay between HpLA concentrations of 40 ng mL^{-1} and 1.25 μg mL^{-1} in HPWB (Figure S2 in the Supporting Information). The IC_{50} value of HpLA was not determined because of the synergic effects, but the IC_{50} of HpKdoLA in IL-6 inhibition was determined to be 340 ng mL^{-1} (Figure S2 in the Supporting Information).

On the other hand, all the synthesized *H. pylori* lipid A and Kdo-lipid A compounds showed IL-18-inducing activity (Figure 1G and 1H). **HpLA** showed the strongest inducing activity for IL-18. In addition, all of the synthetic compounds showed potent IL-12-inducing activity relative to the *E. coli* LPS (Figure S1A in the Supporting Information). The lipid A compounds, **HpLA** and **HpLAEA**, showed stronger IL-12-inducing activity than the corresponding Kdo-lipid A compounds **HpKdoLA** and **HpKdoLAEA**.

HpLA was shown to be the most potent IL-18 and IL-12 inducer, whereas the same compound inhibited IL-1β, IL-6, and IL-8 induction.

Discussion

Recent studies have suggested several pathological implications of bacterial LPS due to their influence on the host immune responses. Synthetic studies of lipid A and LPS partial structures have contributed to investigations of the relationships of structures and functions of LPS, but these relationships are still not well understood. To address this issue, we established an efficient synthetic strategy that is widely applicable to the synthesis of various lipid A compounds, as well as that of lipid A compounds containing Kdo moieties. The strategy (Schemes 1 and 2) employs a key disaccharide intermediate with selectively cleavable protecting groups at the 1-*O*-, 2-*N*-, 3-*O*-, 2′-*N*-, 3′-*O*-, 4′-*O*-, and 6′-*O*-positions for the synthesis of *H. pylori* lipid A compounds (**HpLA** and **HpLAEA**) and Kdo-lipid A compounds (**HpKdoLA** and **HpKdoLAEA**). Natural *H. pylori* LPS have shown only very low endotoxic activity, so low activities or the absence of immunostimulating activities would be expected for the synthetic compounds. A bioassay clearly indicated that **HpLA**, **HpKdoLA**, and **HpKdoLAEA** acted as antagonists against LPS with respect to induction of IL-1β, IL-6, and IL-8. On the other hand, the ethanolamine-form lipid A **HpLAEA** showed weak activity in inducing IL-1β, IL-6, and IL-8. In the previous reports, **HpLAEA** showed immunostimulating activity through TLR4.[55] In these inhibition assays, synergic enhancement effects were observed with **HpLAEA** (Figure 1B, 1D, and 1F) and with **HpLA** (Figure S2 in the Supporting Information) in combination with *E. coli* LPS. Phenomena of this kind have also previously been observed with mixtures of the TLR4 agonist (synthetic *E. coli* lipid A, compound 506) and the strong antagonist (synthetic lipid A precursor IVa, compound 406), in which a mixture of both compounds showed higher biological activities than the agonist itself in an inflammatory cytokine induction assay.[56] We also observed similar effects with mixtures of weak antagonists (lipid A analogues) and a strong agonist (*E. coli* LPS).[29] In natural LPS, one Kdo residue is attached to lipid A, so a natural *H. pylori* LPS with a triacylated lipid A should function as an antagonist in the induction of IL-1β, IL-6, and IL-8 through TLR4.

An important finding is that the presence of a Kdo residue altered the activity of the lipid A compound **HpLAEA**. Several reports, including our own studies, have indicated that Kdo residues enhance the activities of lipid A compounds.[57] However, no synthetic studies have previously reported a transition from immunostimulating to antagonistic activity (or vice versa) through the introduction of a Kdo moiety. The molecular basis for the different activities is presumably due to the differences in charge: **HpLA**, **HpKdoLA**, and **HpKdoLAEA** are anionic, whereas **HpLAEA** is neutral. The difference in charge probably affects the binding of the lipid A part of the structure to the MD-2/TLR4 complex and consequently elicits different responses. Another important finding is that all four synthesized LPS partial structures, **HpLA**, **HpKdoLA**, **HpLAEA**, and **HpKdoLAEA**, are potent inducers of IL-18 and IL-12 in human peripheral whole blood (HPWB). In this case, the presence of Kdo decreased the potencies of the activities. These results clearly indicated that IL-18 and IL-12 were induced by *H. pylori* lipid A and Kdo-lipid A by pathways that differed from the IL-1β, IL-6, and IL-8 pathways activated by *E. coli* LPS. *E. coli* LPS is a potent inducer of the MyD88-dependent pathway factors, such as TNF-α, IL-1β, IL-6, and IL-8, through activation of NF-κB. **HpLA**, **HpKdoLA**, and **HpKdoLAEA** were antagonistic to the induction of these factors and selectively activated the IL-18 and IL-12 pathways.

IL-18 was originally identified as a potent inducer of interferon-γ (IFN-γ)[21] and has recently been shown to play a role in the regulation of Th1 and Th2 responses,[58,59] as well as providing a link between IL-12 and IL-18 in the regulation of IFN-γ production.[60] IL-18 is produced from pro-IL-18 through activation with caspase-1. However, the activation pathway of caspase-1 from procaspase-1 remains a matter of debate. Nakanishi et al. reported that caspase-1 is activated by NALP3 through a TLR4- and TRIF-dependent pathway and leads to IL-18 activation in Kupffer cells.[61] Nuñez et al., on the other hand, described a TLR4-independent caspase-1 activation pathway.[62] More precisely, their research indicated that NALP3 is essential for caspase-1 activation and that the NALP3-mediated caspase-1 activation proceeds independently of TLR signaling (TLR2 and TLR4), the activation instead being mediated by pannexin-1, a hemichannel protein that interacts with the P2X7 receptor.[62,63] Our results and these reports indicated that IL-18 induction by LPS was independent of a NF-κB activation pathway, although the pathways activated by *H. pylori* lipid A and LPS have not been clarified. In contrast, IL-12 secretion was reported to be MyD88-dependent.[64] **HpLA**, **HpKdoLA**, and **HpKdoLAEA** suppressed the induction of MyD88-dependent cytokines, such as IL-1β, IL-6, and IL-8, suggesting the presence of a MyD88-independent pathway for the induction of IL-12.

Cytokine induction by *H. pylori* LPS partial structures demonstrates that these four types of structure either do not induce or induce very low levels of the inflammatory cytokines IL-1β, IL-6, and IL-8 through NF-κB stimulated by hTLR4/MD-2. However, they simultaneously induce high levels of IL-12 and IL-18. This phenomenon could give rise to strong effects on chronic inflammatory reactions, providing a link to atherosclerosis and other inflammatory diseases. The induction of both IL-18 and IL-12 would initiate Th1 cell development, and might be related to the finding that *H. pylori* colonization is inversely associated with childhood asthma.[65]

Conclusion

In this study we have established efficient methods for the synthesis of various lipid A and Kdo/lipid A compounds and have developed the α-selective glycosylation of Kdo and lipid A backbone through application of a microfluidic reaction. Using these newly developed methods, we succeeded in the synthesis of the *H. pylori* LPS partial structures **HpLA (1)**, **HpLAEA (2)**, **HpKdoLA (3)**, and **HpKdoLAEA(4)**, including the first total synthesis of **HpKdoLAEA (4)**. The immunomodulatory activities of these synthesized compounds revealed important links to the virulence of *H. pylori* LPS. Namely, the results reported here are fundamental to the understanding of the molecular basis for the characteristic bioactivities of *H. pylori* LPS, especially with respect to cytokine induction by the lipid A-Kdo structures (including higher induction of IL-18), which are closely related to their virulence expression. In this study we have focused on the synthesis of triacylated compounds. Boons et al. synthesized tetraacylated lipid A compounds derived from *P. gingivalis* and showed that the synthetic lipid A compounds are antagonistic in humans.[37] They also reported the antagonism of *Rhizobium sin-1* lipid A, with a 2-aminogluconolactone and a very long chain fatty acid (27-hydroxyoctacosanoic acid) lacking phosphate.[66,67] Piecing together our results and theirs, the lipid A compounds from these bacteria containing long-chain fatty acids but with smaller overall numbers of acyl groups show antagonistic activity in humans. Our synthetic methods in this report are widely applicable for the synthesis of various kinds of lipid A compounds, and we have recently applied them for the synthesis of tetraacylated *H. pylori* lipid A (aminoethanol phosphate-type) and *Porphyromonas gingivalis* lipid A compounds (tri-, tetra-, and pentaacylated). The immunomodulatory activities, especially IL-12- and IL-18-inducing activities, of these parasitic bacterial lipid A compounds will also be revealed with the synthetic compounds.

Experimental Section

General procedures: ^{1}H NMR spectra were recorded in the solvents indicated with JEOL JNM-LA 500, JEOL ECA 500, Varian INOVA 600, or Bruker AVANCE III 400 spectrometers. The chemical shifts in $CDCl_3$ are given in the form of δ values from tetramethylsilane (TMS) as an internal standard. For measurement in D_2O, the HDO signal (4.718 ppm at 30°C) was used as a reference. ESI-TOF mass spectrometry was carried out with an Applied Biosystems Mariner Biospectrometry Workstation. ESI-IT mass spectrometry was carried out with a Bruker amaZon SL-k1 instrument. High-resolution mass spectrometry was performed with a Waters Q-Tof *micro* (ESI-QTOF) instrument. Elemental analyses were performed with a Yanaco CHNcorder MT-6. Silica gel column chromatography was carried out with Kieselgel 60 (Merck, 0.040–0.063 mm) or Silica Gel 60 N (Kanto Chemical, spherical, neutral, 0.040–0.050 mm) at medium pressure (0.2–0.4 MPa). Gel permeation chromatography (GPC) was carried out with Sephadex LH20 at atmospheric pressure. Precoated Kieselgel 60 F 254 (Merck, 0.5 mm) was used for preparative thin layer chromatography. TLC analysis was performed on silica gel 60 F_{254} (Merck) and compounds were visualized by use of UV (254 nm), phosphomolybdic acid solution (5.0% in EtOH), *p*-methoxybenzaldehyde (0.03%) in EtOH/conc. H_2SO_4/acetic acid buffer or ninhydrin (0.2%) in EtOH/collidine/acetic acid buffer. MS (4 Å and 3 Å) were activated by heating at 250°C in vacuo for 3 h before use. Unless otherwise stated, all reactions were performed at room temperature. Non-aqueous reactions were carried out under argon unless otherwise noted. Anhydrous CH_2Cl_2 was distilled from calcium hydride. Anhydrous THF and CPME were purchased from Kanto Chemicals Japan. Anhydrous DMF was purchased from NACALAI TESQUE, Japan. Distilled water was purchased from Otsuka (Japan) or prepared by use of a combinations of Arium 611 UV (Sautorius) or Toray Pure LV-308 (Toray) and GSL-200 (Advantec, Japan). All other reagents and solvents used were also purchased from commercial sources.

Synthesis of *H. pylori* Kdo-lipid A (20)—batch reaction

Allyl 2-allyloxycarbonylamino-4-*O*-benzyl-6-*O*-[6-*O*-[(benzyl 7,8-di-*O*-benzyl-3-deoxy-4,5-*O*-isopropylidene-α-D-*manno*-oct-2-ulopyranosid)onate]-4-*O*-benzyl-2-deoxy-3-*O*-(4-methoxyphenylmethyl)-2-(2,2,2-trichloroethoxycarbonylamino)-β-D-glucopyranosyl]-2-deoxy-α-D-glucopyranoside (20): A solution of TBSOTf (15.6 μL, 68.0 μmol) in dry CPME (300 μL) was added at 0°C to a mixture of the imidate donor **6** (489 mg, 680 μmol), the acceptor **19** (146 mg, 136 μmol), and MS (4 Å) in dry CPME (2.2 mL) and the mixture was stirred under Ar for 20 min. After addition of saturated aqueous $NaHCO_3$, the mixture was extracted with $CHCl_3$. The organic layer was washed with saturated aqueous $NaHCO_3$ and brine, dried over anhydrous Na_2SO_4, filtered, and concentrated in vacuo. The residue was purified by silica gel flash column chromatography (toluene/EtOAc 20:1→10:1→3:1) to give **20** as a white solid (150 mg, 70%). ^{1}H NMR (500 MHz, $CDCl_3$): δ = 7.31–7.17 (m, 32H; C_6H_5-CH_2-, CH_3O-C_6H_4-CH_2-, C_6H_5-CH_2-OCO-), 6.83 (d, J = 8.5 Hz, 2H; CH_3O-C_6H_4-CH_2-), 5.85 (ddd, J = 22.6, 10.7, 5.6 Hz, 1H; -OCH_2-CH=CH_2 of Alloc group), 5.75 (ddd, J = 22.5, 10.9, 5.7 Hz, 1H; -OCH_2-CH=CH_2 of allyl group), 5.25 (dd, J = 17.2, 1.3 Hz, 1H; -OCH_2-CH=CH_2 of Alloc group), 5.20–5.11 (m, 6H; -OCH_2-CH=CH_2 of Alloc and allyl groups, C_6H_5-CH_2-OCO-), 5.05 (dd, J = 10.5, 9.3 Hz, 1H; H-3), 5.01–4.98 (m, 2H; 2-NH, C_6H_5-CH_2-OCO-), 4.89 (brs, 1H; 2′-NH), 4.73 (d, J_{gem} = 11.2 Hz, 1H; C_6H_5-CH_2-), 4.71 (d, J = 2.7 Hz, 1H; H-1), 4.68 (d, J_{gem} = 10.8 Hz, 1H; C_6H_5-CH_2-), 4.66 (d, J_{gem} = 9.0 Hz, 1H; CH_3O-C_6H_4-CH_2-), 4.63 (d, J_{gem} = 11.3 Hz, 2H; C_6H_5-CH_2-), 4.58 (d, J_{gem} = 11.0 Hz, 1H; CH_3O-C_6H_4-CH_2-), 4.57 (d, J_{gem} = 12.6 Hz, 2H; C_6H_5-CH_2-), 4.51–4.44 (m, 6H; C_6H_5-CH_2-, -OCH_2-CH=CH_2 of Alloc group, -COO-CH_2-CCl_3), 4.41–4.36 (m, 2H; H-1′, H-4″), 4.33 (dd, J = 7.0, 1.3 Hz, 1H; H-5″), 4.06 (d, J = 10.5 Hz, 1H; H-7″), 4.01 (dd, J = 13.0, 5.2 Hz, 1H; -OCH_2-CH=CH_2 of allyl group), 3.98 (dt, J = 4.5, 2.0 Hz, 1H; H-5), 3.96–3.91 (m, 1H; H-2), 3.84–3.81 (m, 2H; H-6a, H-6″), 3.79–3.65 (m, 10H; H-3′, H-8″a, CH_3O-C_6H_4-CH_2-, H-6b, H-4′, H-6′a, H-4, -OCH_2-CH=CH_2 of allyl group), 3.59 (dd, J = 13.5, 3.2 Hz, 1H; H-8″b), 3.37 (t, J = 9.2 Hz, 1H; H-5′), 3.34–3.28 (m, 2H; H-6′b, H-2′), 2.57 (dd, J = 14.9, 5.0 Hz, 1H; H-3″a), 1.90 (dd, J = 14.9, 5.0 Hz, 1H; H-3″b), 1.33 (s, 3H; methyl group of isopropylidene), 1.27 ppm (s, 3H; methyl group of isopropylidene); HRMS (ESI-Q-TOF, positive): *m/z*: calcd for $C_{84}H_{93}Cl_3N_2O_{23}$ $[M+Na]^+$: 1625.5132; found: 1625.5127.

Representative microfluidic reaction procedure for the synthesis of 20: Dry CPME was injected into the micromixer by syringe pump in advance and saturated the microfluidic system. Subsequently, a solution of the donor **6** (48.0 mg, 66.7 μmol, 0.15 M) and the acceptor **19** (48.0 mg, 44.4 μmol, 0.10 M) in CPME (500 μL) and a solution of TBSOTf (9.8 μL, 44.4 μmol, 0.10 M) in CPME (500 μL) were injected to the IMM micromixer, each by syringe pump at a flow rate of 0.5 mL min^{-1}, and mixed at 0°C. After the reaction mixture had been allowed to flow through a stainless reactor tube (Φ = 1.0 mm, l = 25 cm) at 0°C for 42 s, the mixture was added dropwise to saturated aqueous $NaHCO_3$ at 0°C. The mixture was extracted with $CHCl_3$, washed with saturated aqueous $NaHCO_3$ and brine, dried over Na_2SO_4, filtered, and concentrated in vacuo to give the crude product. The residue was purified by silica gel flash column chromatography (toluene/EtOAc 20:1→10:1→3:1) to give the trisaccharide **20** (51 mg, 72%) and the stereoselectivity was analyzed by ^{1}H NMR spectroscopy (α/β > 95:5).

Other syntheses and spectroscopic data are shown in the Supporting Information.

